AIR FORCE INSTITUTE OF TECHNOLOGY

AIR UNIVERSITY
UNITED STATES AIR FORCE

A TWO ELECTRODE ELECTROCHEMICAL SENSOR
FOR DETECTING TRACE PROPELLANTS IN AIR

THESIS

GE/EE/63-19 Paul C. McLellan, Jr.
Capt USAF

SCHOOL OF ENGINEERING

WRIGHT-PATTERSON AIR FORCE BASE, OHIO

AF-WP-O-OCT 62 3,500

A TWO ELECTRODE ELECTROCHEMICAL SENSOR FOR DETECTING TRACE PROPELLANTS IN AIR

THESIS

Presented to the Faculty of the School of Engineering of
the Air Force Institute of Technology
Air University
in Partial Fulfillment of the
Requirements for the Degree of
Master of Science in Electrical Engineering

By

Paul Curtis McLellan, Jr.

Capt USAF

Graduate Electrical Engineering

August 1963

Preface

The investigation reported in this thesis is based upon a proposal by Dr. N. A. Poulos of the Toxic Hazards Branch, Aerospace Medical Research Laboratories, Wright-Patterson AFB, Ohio. Although the basic sensor described in this thesis is the same as the one used by Dr. Poulos in his report on the Amperometric Propellant-Component Detector, the research of this report differs in two important respects: first, different electrolytic dip solutions are used with the sensor, and second, the sensor response is optimized through an analysis of its electrical equivalent model.

The author acknowledges his indebtedness to his thesis advisor, Capt. Matthew Kabrisky, for his pertinent suggestions and assistance in the preparation of this thesis and to Dr. Poulos for his intense interest and professional knowledge. Thanks are due two other members of the Toxic Hazards Branch: first, Lt. Duncan McVean for his ideas on the philosophy of the subject, and second, Airman Joseph Miller for his invaluable laboratory assistance. Special thanks are given to the author's wife for her moral support and typing of the original manuscript.

Paul C. McLellan, Jr.

Contents

	Page
Preface	ii
List of Figures	v
List of Tables	vi
Abstract	vii
I. Introduction	1
Background	1
The Problem	2
General Method of Detection	2
Assumptions - Limitations	3
Issues - Method of Solution	4
II. Theory	5
Flow of Electric Current	5
Cell Capacitance and Electrical Double Layer	7
Cell Electrical Model	8
Effect of UDMH	11
III. Experimental Techniques	12
Measurement of Electrical Parameters	12
Measurement of Cell Response to UDMH	15
IV. Experimental Results	20
General	20
KI Electrolyte	21
KCl Electrolyte	30
KBr Electrolyte	31
Summary of Results	37
V. UDMH Equivalent Circuit	39
VI. Conclusions - Recommendations	47
Bibliography	48

Contents

Page

Appendix A: Determination of UDMH Concentration in Air . . . 49

Appendix B: Sample Calculations 52
Cell Capacitance 52
Characteristic Curve 54
UDMH Approximations 55

Appendix C: Construction of Cells and Composition of Electrolytic Solutions 59

Appendix D: Optimization of Cell Parameters 61

Vita 62

List Of Figures

Figure		Page
1	Electrical Double Layer	7
2	Electrical Equivalent Circuit for Cells	8
3	Block Diagram for Circuits used to Determine Electrical Characteristics	13
4	Flow Apparatus	17
5	Schematic of Flow System	18
6	Typical Characteristic Curve (Cell Y)	22
7	Characteristic Curve Cell X	23
8	Characteristic Curve with KI Dip Solution Showing Dependence on Time of Dip	24
9	Variation of Cell Y Resistance with Increasing I_p	25
10	Change in Cell Voltage as a Function of UDMH Concentration (KI)	28
11	Dependence of Characteristic Curve on Time of Dip	32
12	Change in Cell Voltage as a Function of UDMH Concentration (KBr)	35
13	Typical Response-Recovery Curve	40
14	Cell Equivalent Circuit for UDMH	41
A1	Apparatus For Determination of UDMH in PPM	50
A2	Concentration of UDMH in PPM in Air versus Per Cent UDMH in 2 Per Cent NaOH Solution	51
B1	Experimental and Theoretical Time Response to Step Input	56
B2	Linear Approximation of Cell Response	58
C1	Cells	60

List Of Tables

Table		Page
I	AC Resistance and Capacitance in KI Electrolyte	26
II	Response Time Constants for KI Electrolyte	27
III	Recovery Time Constants for KI Electrolyte	29
IV	Overvoltage Deviation with KCl Electrolyte	30
V	Response to 0.5 PPM UDMH and Blank in KCl Electrolyte .	31
VI	AC Resistance and Capacitance of Cells in KBr Electrolyte	33
VII	Comparison of Capacitance at Two Frequencies in KBr ..	33
VIII	Response Time Constants for KBr Electrolyte	36
IX	Recovery Time Constants for KBr Electrolyte	36
X	Comparison of Calculated ΔE with Experimental ΔE	46

Abstract

The accurate detection of UDMH to its threshold limit value is achieved with a two-electrode-electrochemical sensor and a KI electrolyte. Three electrolytes are tested with two cells to realize this detector. The theory of electrochemical reactions in solutions is valid for this sensor, and the large capacitance is explained by the electric double layer concept. An equivalent electrical model is derived to optimize sensor response. A flow system and standard measuring instruments are used to obtain the experimental results. The electrochemical reaction between the cell and UDMH results in a decrease of overvoltage in proportion to the concentration of UDMH in air. Finally, a linear approximation of this reaction is obtained with a UDMH equivalent circuit.

GE/EE/63-19

A TWO ELECTRODE ELECTROCHEMICAL SENSOR FOR DETECTING TRACE PROPELLANTS IN AIR

I. Introduction

Background

Detecting systems for many trace contaminants have been successfully used for years. However, the accuracy of current methods for detecting Unsymmetrical Dimethyl Hydrazine (UDMH) is not adequate. Also, these devices have experienced difficulties with baseline drift and baseline return, i.e., return to a reference level. Some attempt has been made to overcome these undesireable characteristics, but the methods employed are complex and have not completely solved the problem (Ref 11:14). UDMH is presently used by the U. S. Air Force as a missile propellant. It is a toxic hazard to man when present in minute quantities in the air he breathes. Exposure to large amounts results in convulsions and possibly death. Therefore, it is essential that the concentration of this propellant in air be detected in a form which is readily and simply accessible. Present devices are not adequate for the protection of personnel. The only known detecting devices for UDMH will not detect its Threshold Limit Value (the minimum safe limit that can be withstood by man with no detrimental effects (Ref 11:19). Consequently, a small, simple inexpensive device is required; an essential part of such a device is the sensor.

The Problem

The purpose of this thesis is to develop, evaluate, and improve an electrochemical sensor for the detection of trace propellants in air. The primary propellant to be considered is UDMH which must be detected in the 0.5 to 5 PPM range. Although the solution of the problem relies mainly on analysis of the electrical parameters of the sensor, an investigation of the electrochemical effects to explain the operation of the cell is necessary. A standard two electrode sensing device is utilized rather than multi-electrode devices. The standard device (cell) consists of two platinum electrodes separated by surgical gauze mounted on polyethylene tubing (Ref 11:3). In addition, none of the following will be considered in the problem: electrode geometry other than the standard, electrode materials other than platinum, and oxidation propellants (UDMH is a fuel or reduction propellant). The investigation of atmospheric disturbances such as temperature, pressure, and humidity will not be attempted. When required, the definitions of new terms and concepts will be given.

General Method Of Detection

The sensor or detector cell is dipped into a suitable electrolytic solution, then withdrawn and exposed to the atmosphere. Three electrolytes are tested with results given in a later chapter. If a trace propellant is present, an electrochemical reaction takes place in the cell and a small change in its potential results. This change

of potential can be amplified, if required, and displayed by a metering arrangement to give the amount of the trace in air with respect to some reference.

Assumptions - Limitations

Before attempting to solve the problem certain assumptions were made to limit its scope. First, it was assumed that the standard cell configuration could be adopted for this detector; second, that one of the three dip solutions would give the desired response; finally, that atmospheric effects will have little or no effect on the cell's response. The configuration proposed has been used successfully to detect contaminants that are similar to UDMH, but has not been able to detect UDMH accurately below 5 PPM (Ref 11:14). However, different dip solutions were used than those tested here. One of the solutions that is tested is an iodine electrolyte which has already been adapted to various electrochemical instruments (Ref 6:8). This electrolyte, involving an iodine-iodide reaction, is one of the few which is practically 100% efficient and is therefore highly adaptable for quantitative use. Possibly the most significant limiting effect is that atmospheric disturbances will not be negligable. These assumptions were proved valid by the experimental results. The small changes in atmospheric conditions that were observed in the laboratory did not seem to effect the cells.

Issues - Method Of Solution

Three basic issues must be resolved. These three are stability, response, and sensitivity. As part of the stability problem, drift, return to reference level, and baseline stability must be determined. Response must be checked within a range of all concentrations of contaminants to be expected. Sensitivity must be such that the lowest levels (Threshold Limit Value) of contaminant can be detected. Sensitivity as used here is defined as the millivolt meter output per one PPM of chemical input in air.

The chosen method to resolve these issues consists of evaluating the three dip solutions after the electrical and electrochemical properties of the two test cells have been determined. Once this has been done, an optimum electrolyte and cell combination can be chosen. This choice is necessary to limit the problem so that an answer can be realized in the time allowed for research. The method will be pursued in the following chapters. Chapter II deals with the general theory of the operation of the cell. Chapter III discusses the techniques used in the experimental measurements. Chapter IV gives the experimental results and compares these results with the theory. Chapter V suggests an equivalent circuit for the cell when exposed to UDMH. Chapter VI consists of conclusions derived from the research and suggests further investigations.

II. Theory

Flow Of Electric Current

The best known type of current flow is through metallic conductors while current flow through electrolytic conductors is less familiar and is most generally studied in the field of electrochemistry. In electrolytic conduction, the carriers are much larger than the electrons which move in solid conductors and are of atomic or molecular size. Each of these carriers or ions may possess a positive (cations) or negative (anions) charge in the solution. These ions are created by the dissociation or separation of the molecules of a chemical agent when it is dissolved in a suitable solvent such as water. An example, potassium bromide (KBr) dissolved in water is used as a dip solution. This salt dissociates into positively charged potassium ions (K^+) and negatively charged bromide ions (Br^-).

$$KBr \rightarrow K^+ + Br^- \qquad (2\text{-}1)$$

This is termed an "electrolytic solution" and the dissolved KBr is an "electrolyte".

When an electric field is present between two electrodes immersed in an electrolytic solution, the cations move to the negative electrode while the anions move to the positive electrode producing a total current which is the sum of the individual currents due to the moving ions (Ref 6:5). The rate at which these ions move through the solution, their number, and the potential obtained at the electrodes due to the discharge of ions determines the conductance of the electrolyte (Ref 5:557).

Since the electrodes of the detector cells are not in a solution but are separated by electrolytically wetted surgical gauze, they may be thought of as immersed in a less than ideal electrolytic system. However, the general theory of the electrochemical processes which take place remain unchanged in this environment. The detector cells are reversible, that is to say, they will support a flow of current in either direction. The reversible potential is the potential at equilibrium, or at minimum current flow through the cell. Any potential which is in excess of this reversible potential is defined as overvoltage, and the cell is said to be polarized (Ref 10:124).

There is also a definite relationship between the amount of current passing through the cell and the chemical changes which take place at the electrodes. This relationship, called Faraday's law, states that 96,500 coulombs flowing across a metal-electrolyte boundary will reduce or oxidize one gram-equivalent weight of the reactant (Ref 10:8). Thus the amount of reactant formed can be expressed by:

$$g = \frac{(\text{coulombs passed})(\text{eq. wt. of reactant})}{(\text{value of Faraday})} \qquad (2\text{-}2)$$

where g is grams of reactant. At a polarizing current of 100 micro-amps, Faraday's law shows that it would take 2,100 hours to deposit one gram of iodine at the positive electrode of the cell.

Cell Capacitance And Electrical Double Layer

A distribution of ions called the electrical double layer exists at the boundary of any solid and solution. This is shown in Fig. 1 for one electrode.

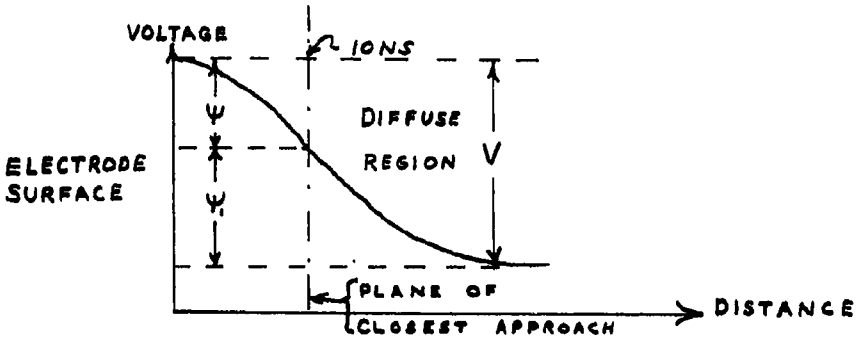

FIG. 1 ELECTRICAL DOUBLE LAYER (REF 7:361; 2:822)

The voltage change across the double layer consists of a section Ψ from the electrode to the plane of closest approach (Helmholtz layer) and Ψ' in the diffuse region (Guoy layer) such that $V = \Psi + \Psi'$. The ions at the plane of closest approach are closely bound to the electrode surface while the ions in the diffuse region are free to move (Ref 2:820-2). Note this implies that the charge and therefore capacity of the electrode is dependent upon the voltage. This double layer of charge is analogous to a charged parallel plate condensor (especially in the compact Helmholtz layer) and is chiefly responsible for the large capacitance of the detector cell (Ref 7:590). A calculation of the capacitance

of the cell (X) from field theory shows that it is on the order of 2000 μμf, while experimental determination shows that it is on the order of 200 μf (See Appendix B). The thickness of the Helmholtz layer is nearly constant for all systems, and therefore the capacitance due to this layer should be nearly constant for the electrolytes used. There are various methods offered (Ref 8:552) which lead to the theoretical determination of cell capacitance which utilize electrode kinetics or ionic studies, but these can be used only with concentrated solutions and do not appear to be applicable to the detector cells. In addition, the equation derived for the voltage response in the following section leads to a simple, accurate determination of the cell capacitance.

Cell Model

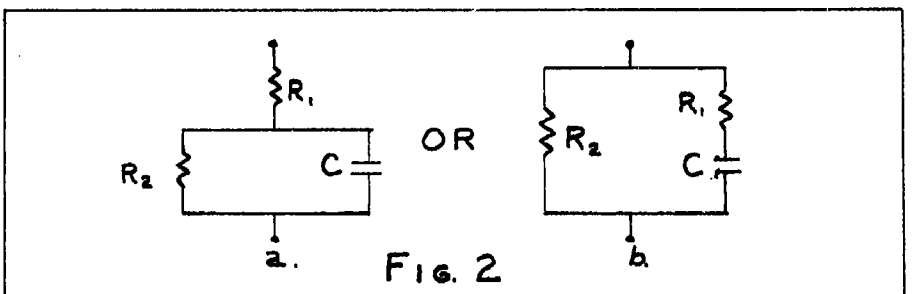

FIG. 2

ELECTRICAL EQUIVALENT CIRCUIT FOR CELLS

The equivalent circuit for the detector cells is shown in Fig. 2 above. The experimental determination of this model is given in

Chapter IV Experimental Results. Assuming a constant current source input and neglecting R_1, since $R_2 >> R_1$, to simplify the solution, the circuit becomes:

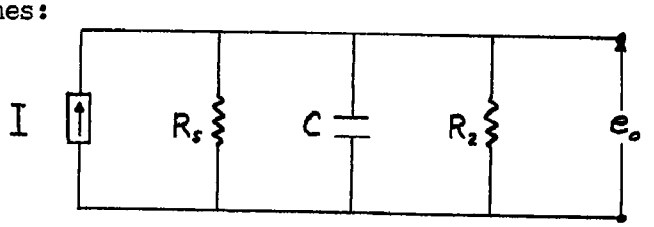

This is equivalent to:

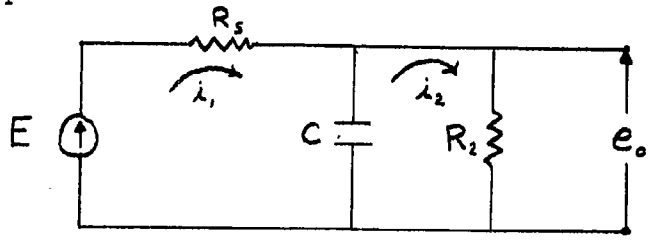

(This equivalent source is used since it is the same as that used in the experimental determinations of the model.)

Thus
$$\left(R_s + \frac{1}{CD}\right) i_1 - \frac{1}{CD} i_2 = E \qquad (2-3)$$

$$-\frac{1}{CD} i_1 + \left(R_2 + \frac{1}{CD}\right) i_2 = 0 \qquad (2-4)$$

Solving (2-3) and (2-4) for i_2:

$$i_2 = \frac{\dfrac{E}{R_s R_2 C}}{D + \dfrac{R_s + R_2}{R_s R_2 C}} \qquad (2-5)$$

Now let E be a step function and taking the Laplace Transform of (2-5) it becomes:

$$I_2(s) = \frac{\frac{E}{R_s R_2 C}}{S\left(S + \frac{R_s + R_2}{R_s R_2 C}\right)} \qquad \text{LET } \tau = \frac{R_s R_2 C}{R_s + R_2} \qquad (2-6)$$

hence

$$E_o(s) = I_2(s) R_2 = \frac{\frac{E}{R_s C}}{S\left(S + \frac{1}{\tau}\right)} \qquad (2-7)$$

Taking the inverse Laplace of (2-7), the voltage output as a function of time is:

$$e_o(t) = \frac{E R_2}{R_s + R_2}\left(1 - e^{-\frac{t}{\tau}}\right) \qquad (2-8)$$

Also, from (2-7) the transfer function of the cell is:

$$G(s) = \frac{1}{R_s C\left(S + \frac{1}{\tau}\right)} \qquad (2-9)$$

An analysis of equation (2-8) to determine the optimum response of the cell (See Appendix D) indicates the cell capacitance should be made small. This will not effect the final value of the response but will decrease the response time.

Effects Of UDMH (Or Any Reducing Agent)

In the platinum (metallic) portions of the detecting circuits conduction takes place by electrons, while in the solution conduction takes place by ions. Obviously, then, the current carrier must change from electrons to ions or conversely at the electrolyte-metal interface. This change is achieved by an electrochemical reaction which involves gain or loss of electrons. When an electron is gained by the reactant, the reaction is a reduction process, and when an electron is lost by the reactant, it is an oxidation process (Ref 6:6-8).

When the cell is exposed to UDMH, the UDMH yields electrons to the cell; hence, the potential across the cell decreases in proportion to the concentration to which it is exposed. Another theory which explains this drop is potential of the polarized cell when exposed to UDMH or other fuels is the interaction of the fuel with a high resistance PtO (Platinum-oxide) layer on the outer electrode. This causes a large decrease in resistance by "cleaning" the PtO off the electrode causing a corresponding decrease in the cell voltage. This also explains the recovery of the cell by the healing or reforming of the PtO layer under the influence of the externally applied polarizing current. Moreover, the time of healing is directly proportional to the amount of polarizing current applied (Personnal Communication With Dr. N. A. Poulos).

III. Experimental Techniques

Measurement Of Electrical Parameters

Several measurements are required to determine the parameters and characteristics of the cells. These measurements consist of: (1) the D-C resistance, (2) the characteristic (polarization) curves, (3) the AC resistance, and (4) the capacitance. The methods chosen were limited by the equipment available in the laboratory.

AC measurements were made to determine the AC resistance and capacitance. The circuit for these measurements is illustrated in Fig. 3-B. By taking a known resistor R in series with the cell and placing a known sinusoidal voltage across the terminals A-C, the magnitude of the rms voltage across the cell and the current through it can be found. Consequently, the cell resistance and reactance can be calculated with the aid of a phasor diagram. However, knowledge of the reactance and resistance does not indicate whether the reactance is capacitive or inductive; moreover, it will not show whether the resistance and reactance are in series or parallel. The first difficulty is resolved by placing a known capacitance (or inductance) of approximately the same impedance at the frequency of the applied voltage in parallel with the cell. If the cell is inductive (capacitive), the impedance of the cell will rise markedly; if the cell is capacitive (inductive), the impedance will increase (decrease) slightly. These changes in impedance are observed by the proportional

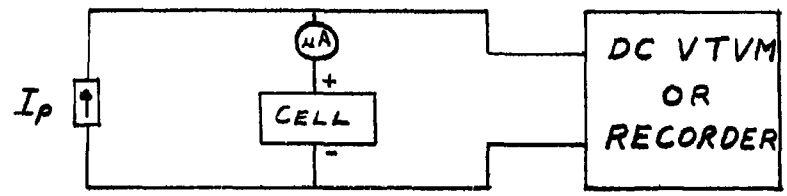

A. Circuit For DC Measurements

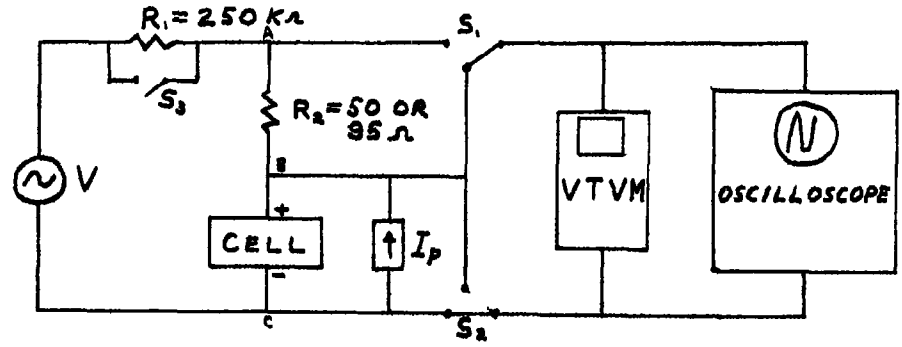

B. Circuit For A-C Measurements

Fig. 3

Block Diagrams For Circuits Used To Determine Electrical Characteristics

changes in voltage measured on a VTVM. The second difficulty is overcome by calculating the capacitance or inductance assuming first, a parallel circuit and second, a series circuit. A comparison with the value calculated from the rise time will indicate which is correct. If the capacitance or inductance is constant, the series or parallel quandry can be resolved by increasing the input frequency and noting the change in the impedance of the cell. For example, if the cell is capacitive and the AC resistance is in series, the impedance will approach that of the resistance as the frequency approaches large values. If, however, the resistance parallels the capacitance, the impedance will approach zero. (The experimental results show that the cell is capacitive and the equivalent circuit is a series circuit.)

Next, the circuit for obtaining the DC resistance, capacity, and characteristic curves of the cells is shown in Fig. 3-A. I_p is varied from 0 to 100 ua in steps to obtain the overvoltage of the cell and thus the characteristic curve. At the same time, the steady-state values of overvoltage are used to obtain the DC resistance. In addition, the rise time between changes in I_p can be used to calculate the time constant of the cell. When the time constant, source resistance, and cell resistance are determined, the capacitance can be caluclated by

$$\tau = RC, \text{ where } R = \frac{R_s R_2}{R_s + R_2} \qquad (3\text{-}1)$$

A sample calculation is given in Appendix B and compared with the value obtained from AC measurements described in the previous

paragraph. Since cell resistance is a function of the polarizing current, I_p, the calculations for capacitance were made where this change in resistance was most nearly constant.

There are certain limitations associated with the measurement techniques described above. First, the AC and DC measurements must be accomplished with solutions having low concentration of impurities (Ref 7:591). Second, inaccuracy may result from the AC measurements because the electrode surface is irregular and gives a variation of capacitance with frequency. There are two reasons for this: first, the medium between the electrodes and the electrodes themselves, do not behave as a simple resistance and capacitance as assumed, and second, the current distribution over the electrode is not uniform (Ref 8:143). However, the methods cited are the most accurate available. (Ref 7:589-91) and will suffice so long as these limitations are remembered. Finally, the resistance of the electrolytes increase with temperature (Ref 4:65) and with time because of a slight variable drying of the gauze. Therefore, some variations will occur in the characteristics of the cells from day to day.

Measurement Of Cell Response To UDMH

The measurement of the cell response to UDMH was attempted by two methods: static and dynamic. The objective of these measurements was to see if UDMH could be detected in the 0.5 to 5 PPM range and if an optimum electrolyte could be obtained. The optimum is defined

as the best electrolyte with respect to stability, response, and return to reference.

The first analytic determinations were made by the static method i.e., by exposing the cell to UDMH contained in a flask above a solution of UDMH and 2% NaOH in water. The purpose of the NaOH is to maintain a linear vapor pressure since UDMH is hygroscopic (Ref 3:90). The static method was continued until the exact concentration of UDMH in air above the NaOH solution was known. The apparatus and method of determining this relationship is given in Appendix A. At this time the static method was discarded and a dynamic or flow system was built. The reasons for this change were: (1) static methods are limited in the PPM range, (2) losses of the test gas in excess of 50% by absorption on the surfaces of the test equipment can be expected (Ref 12:1100), and (3) the number of analytic determinations is limited because only a certain amount of gas (on a volume basis) can be withdrawn unless a very large volume flask is used. In a flow system, the losses are not as serious since a steady state is attained a short time after the system is turned on, and no further losses occur (Ref 12:1100). In addition, the total system is smaller than the static. The flow system is pictured in Fig. 4 and diagrammed in Fig. 5. Referring to Fig. 5 the operation is as follows: first, the split flow valve allows air to flow through the bleeder and into the UDMH solution at the bottom of the 250 ml. flask (bubbler) with a rate (1.22 l/m)

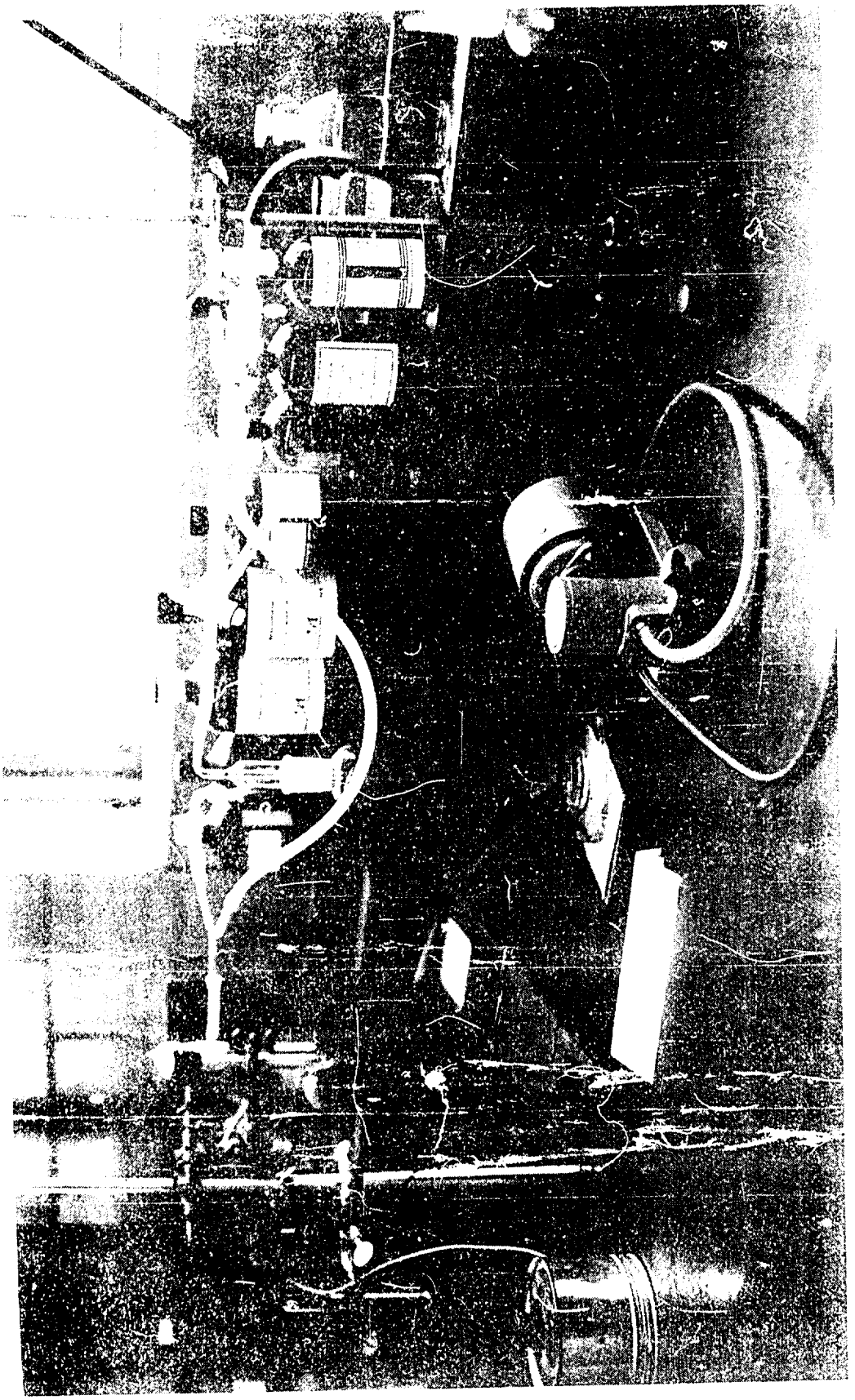

FIG. 4

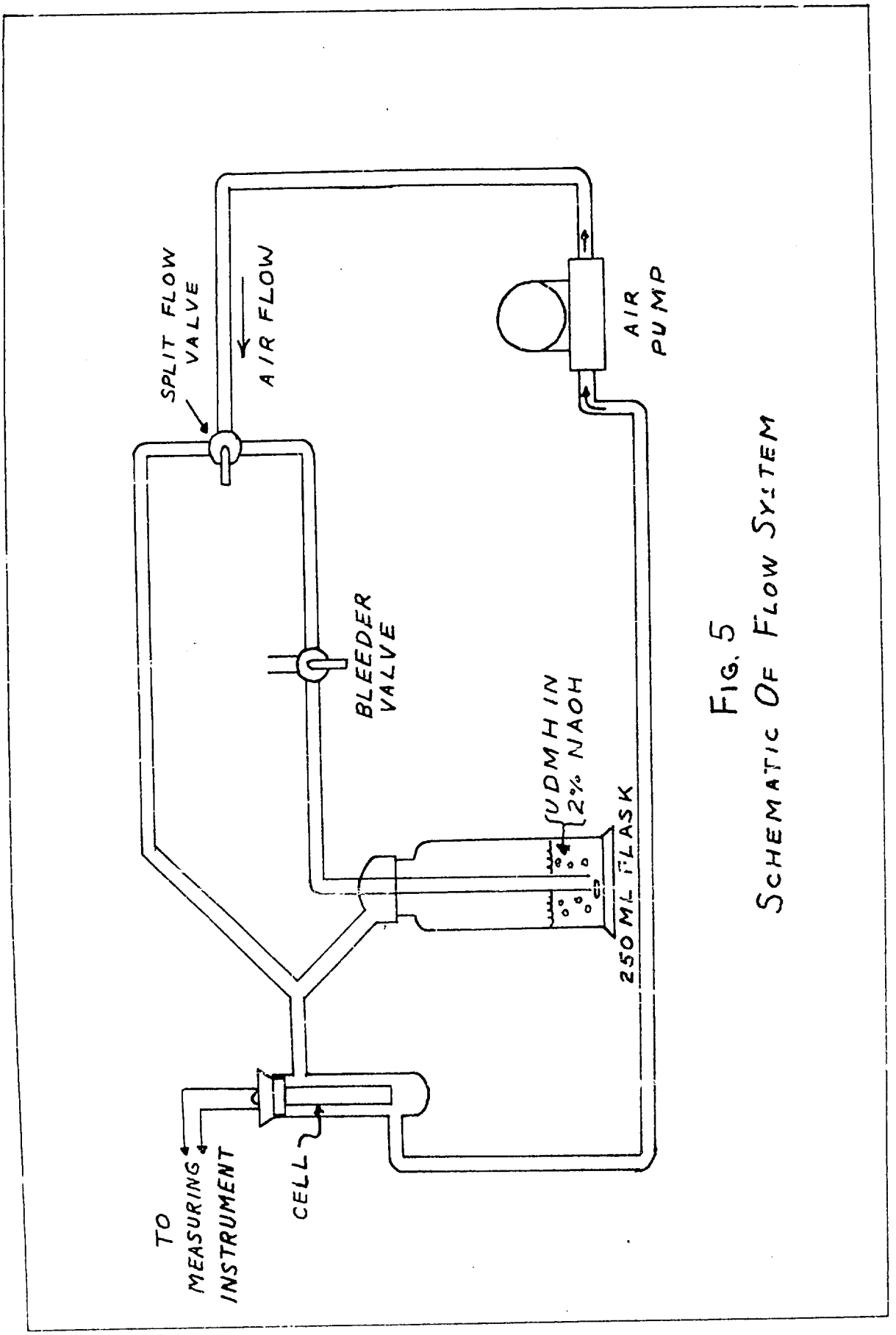

FIG. 5
SCHEMATIC OF FLOW SYSTEM

equal to that used in determining the concentration as described in Appendix A; second, the air-UDMH mixture flows past the cell which responds in proportion to the amount of UDMH present; third, the response is measured by a continuous recorder connected to the cell lead-in wires; fourth, once a steady state is reached, the split flow valve is rotated so that the air flow bypasses the flask; and fifth, the tubing to the suction side of the vacuum pump is removed allowing uncontaminated air to flow by the cell. This process is repeated for all concentrations of UDMH to be detected. Another important measurement made by this method is the response to a blank solution. The blank consists of only the 2% NaOH in distilled water solution. Any response to the blank must be subtracted from the total response to the UDMH.

IV. Experimental Results

General

In many cases the data for the different electrolytes (dip solutions) were quite similar. This is true with respect to the characteristic curves and resistance curves. For the sake of brevity, where marked similarity in the shape of curves occurred for more than one dip, only one graph is shown instead of two or three. For example, only one graph of the variation of cell resistance with polarizing current is shown. Thus, the reader may assume that the resistance of the two cells in the three different electrolytes varied in the same general manner.

Although some of the problems encountered in the experimental work are given in the discussion of the three electrolytes, the problem that gave the most difficulty applies to all three. This was the handling of UDMH. The UDMH was obtained from a 1% stock solution which was in turn diluted with the 2% NaOH, on a volume to volume basis, for the required PPM concentration in air. This dilution had to be accomplished with great accuracy, especially at the lower ranges of UDMH concentration, or repeatability was not achieved. From Fig. A-2 it can be seen that a mixture of 0.01% UDMH in the 2% NaOH solution is required to give 0.5 PPM of UDMH in air. In addition, as UDMH aged its electrochemical reaction with the cells varied. As a result,

the 1% stock solution was used for only five days even though it was kept under refrigeration. All data taken with UDMH older than this was discarded.

The construction of the two cells is described in Appendix C. The smaller cell (Y) was built to verify the theoretical conclusion that response would be improved by decreasing capacitance. The remainder of this chapter presents the experimental results as obtained from the three electrolytes (KI, KCI, KBr).

KI Electrolyte

To determine the polarization curves, the circuit of Fig. 3-A was used. A typical curve of I_p versus E, the reversibility, and hysteresis effect is shown in Fig. 6 for cell "Y". Fig. 7 is the characteristic curve for cell "X". Data were also taken over increased periods of time to see what effects, if any, time of dipping had on the cell. The results of this study, shown in Fig. 8, indicated an increase in cell resistance with time after dip. Since the variation of the characteristics was fairly constant up to four hours (especially at the lower ranges of I_p), all further experimentation was carried out within four hours after the cell was dipped, unless otherwise noted, to minimize error. The DC resistance is calculated by dividing the steady-state voltage (E) across the cell by the steady-state polarizing current (I_p). The variation of R_{DC} with I_p is shown in Fig. 9 for cell "Y".

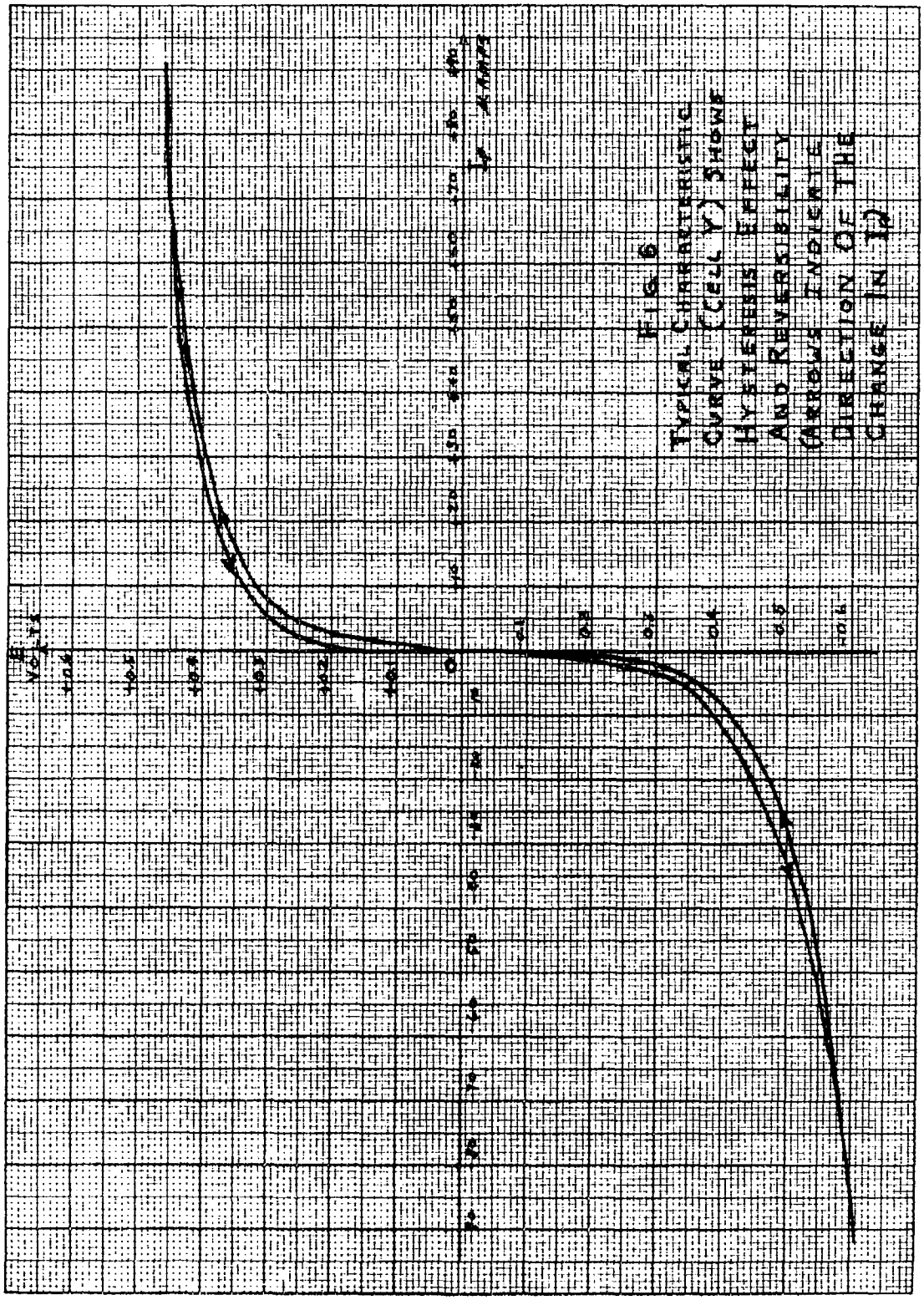

FIG 6
TYPICAL CHARACTERISTIC CURVE (CELL V) SHOWS HYSTERESIS EFFECT AND REVERSIBILITY (ARROWS INDICATE DIRECTION OF THE CHANGE IN I)

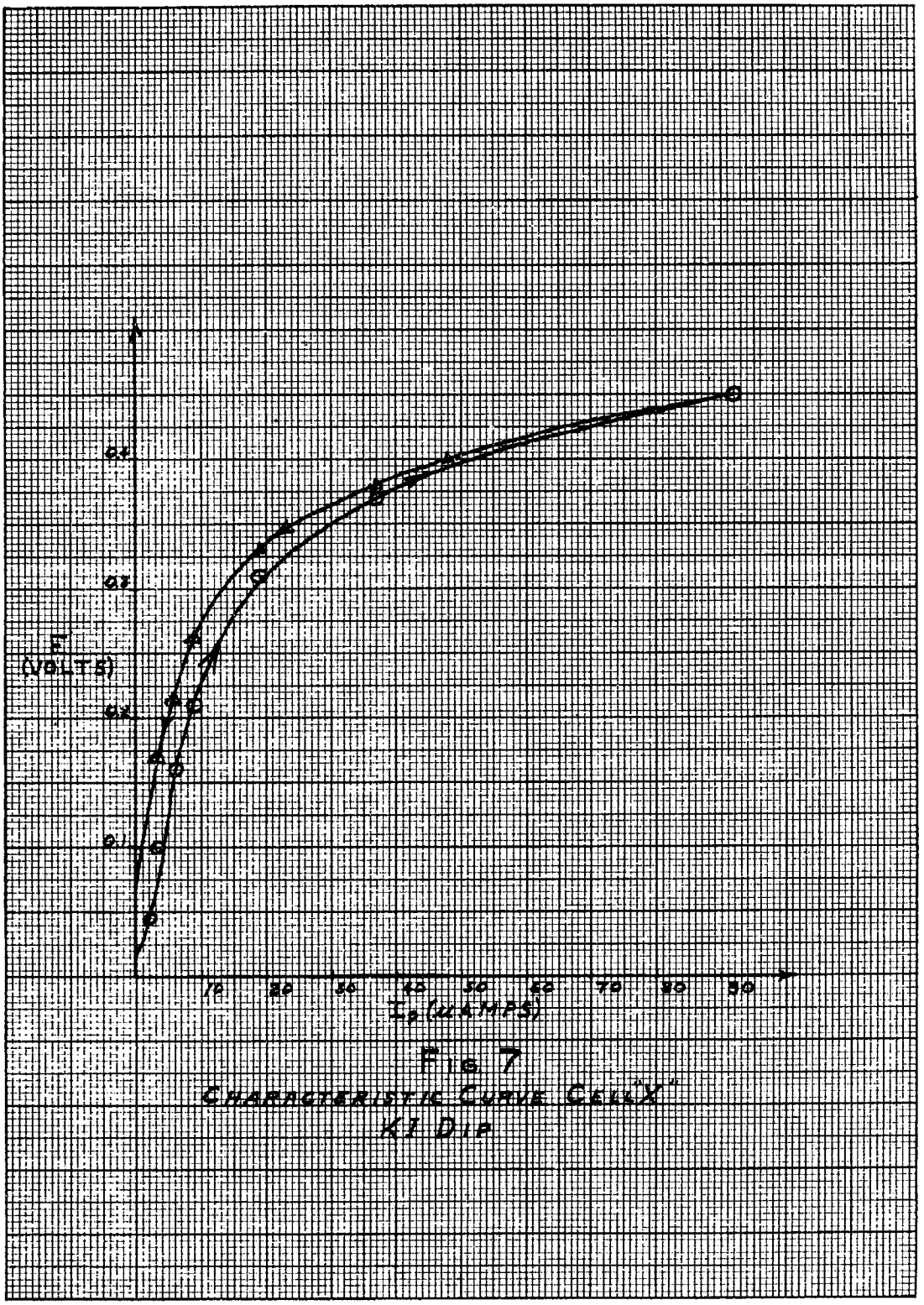

FIG. 7
CHARACTERISTIC CURVE CELL "X"
K1 DIP

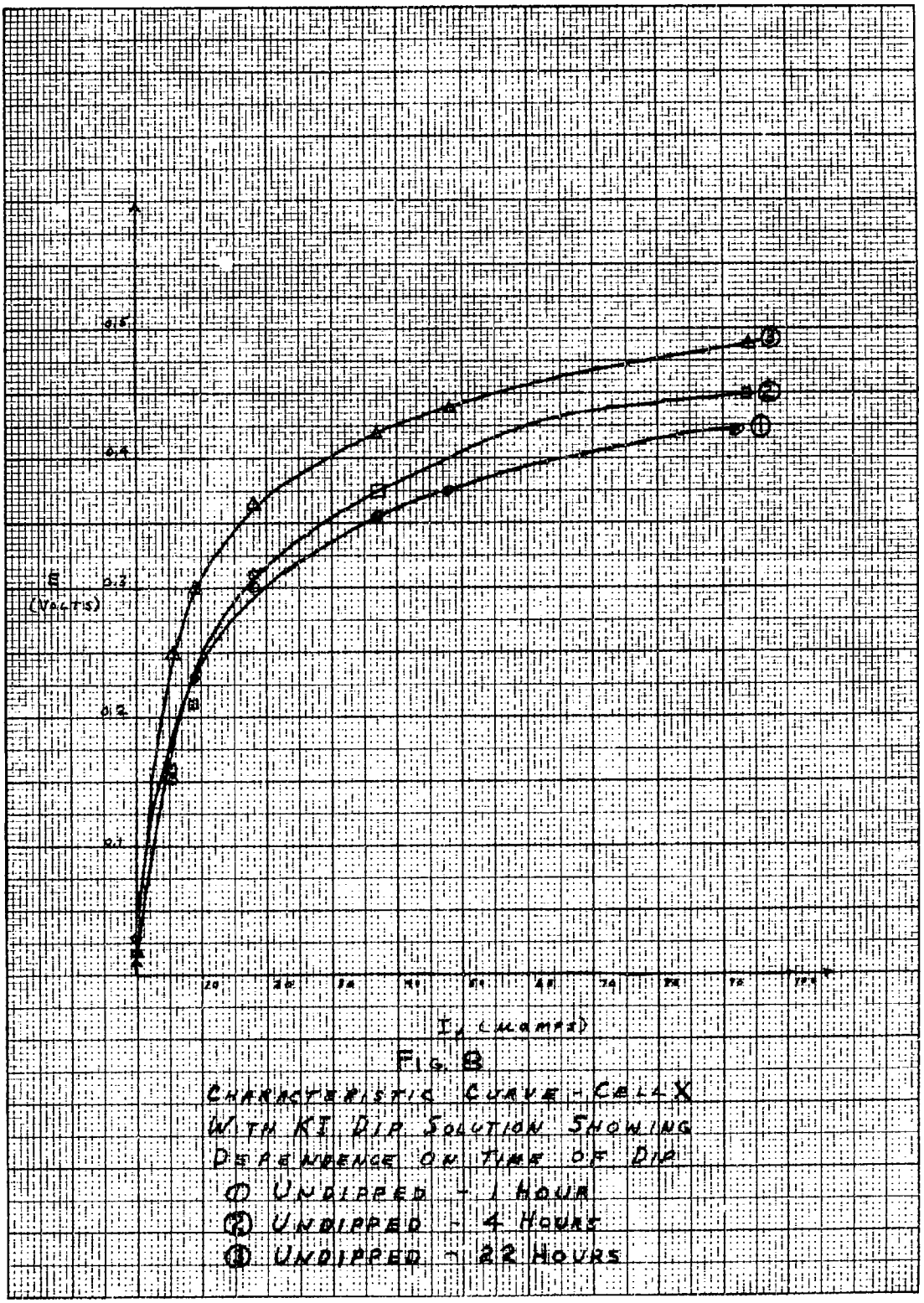

FIG. 8

CHARACTERISTIC CURVE - CELL X WITH KI DIP SOLUTION SHOWING DEPENDENCE ON TIME OF DIP

① UNDIPPED - 1 HOUR
② UNDIPPED - 4 HOURS
③ UNDIPPED - 22 HOURS

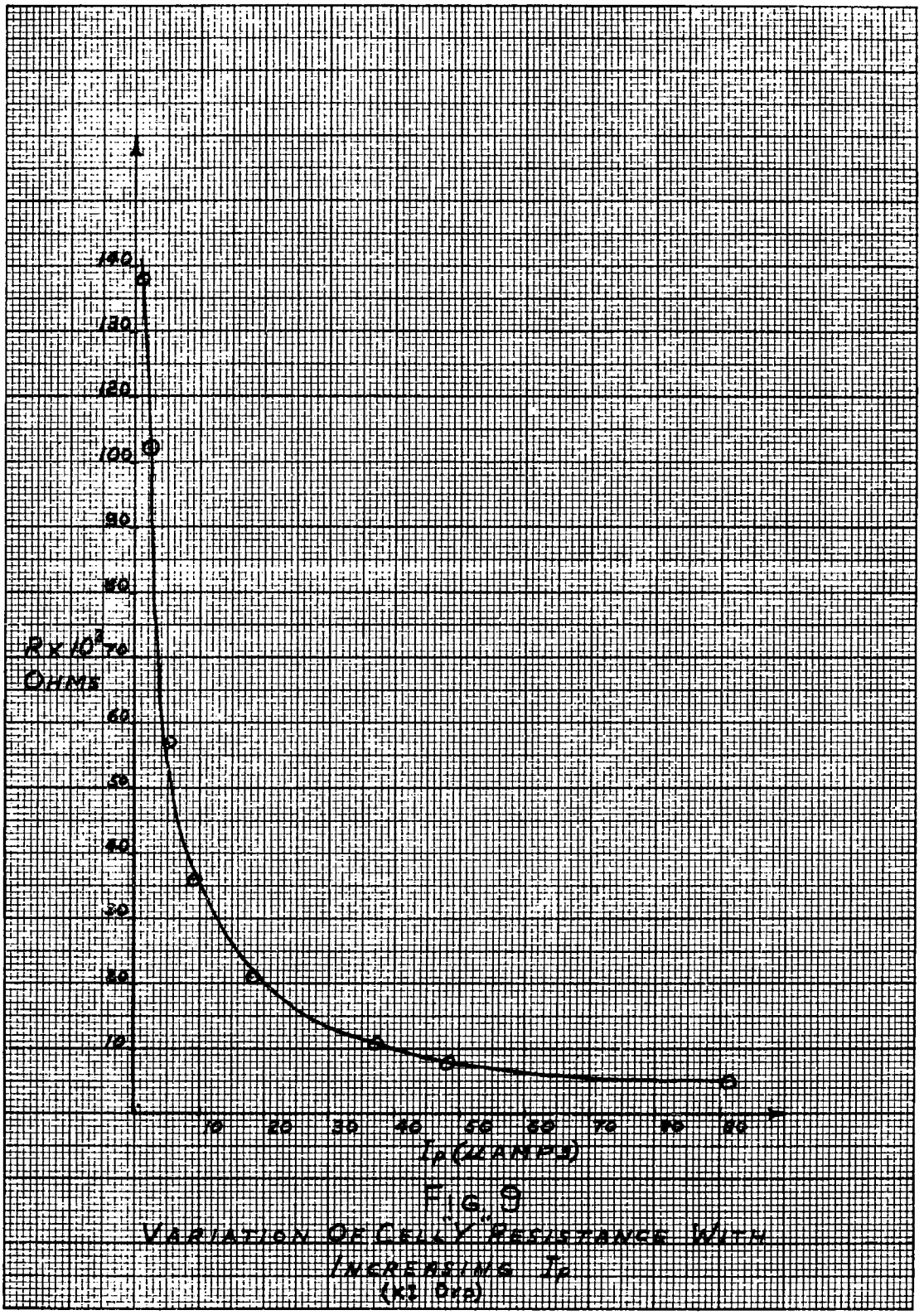

FIG. 9
VARIATION OF CELL'S RESISTANCE WITH INCREASING I_D

Next, AC measurements (Fig. 3-B) were made to determine the capacitance of the cell and AC resistance. First, I_p was varied over its entire range (0 to 100 microamps) while a steady sinusoidal input was applied. Position of switches (Fig. 3-B): S3 open, S1 and S2 in position 2. No noticeable distortion was observed on the oscilloscope; however, the capacitance decreased as the polarization current increased. Second, the response to AC alone was measured by closing S3 and measuring the voltage across R_2, then the cell, after I_p was set to zero. A typical calculation for R_{AC} and C of the cell is given in Appendix B with results given in Table I.

TABLE I

AC Resistance and Capacitance of Cells in KI Electrolyte

T = 22° - 26° C. R = 50 ohms Frequency = 60 cycles

	V_{cell} volts	V_R volts	R_{AC} ohms	C microfarads
Cell "X"	0.480	1.76	9.1	262
	0.325	1.35	7.2	230
	0.262	0.95	7.9	235
	0.290	1.09	7.1	234
Cell "Y"	0.636	0.89	19.0	88
	0.495	0.72	25.2	113
	0.332	0.44	25.8	96
	0.280	0.35	28.2	95
	0.180	0.22	29.7	95

After computing these electrical parameters, cell response to UDMH was evaluated. The response was much slower than that given by the electrical equivalent circuit because of the electrochemical reaction between UDMH and the KI. However, the cell did detect UDMH at its TLV. Table II relates the time constants of this reaction for various values of I_p with cell "X" and cell "Y". Note the improvement in time of response (or T.C.) of cell "Y" over cell "X". The total response is plotted against the concentration of UDMH on a Log_{10} Scale in PPM in Fig. 10. Although the maximum response is obtained at an I_p=5ua, recovery is very slow. At higher values of I_p recovery is appreciably faster as shown in Table III. KI response to the blank was negligable at all levels of polarization used. In addition, return to reference was achieved within ± 1 mv.

TABLE II

Response Time Constants for KI Electrolyte

	Cell "X"		Cell "Y"	
	T.C.[a] at UDMH in PPM		T.C. at UDMH in PPM	
	0.5	0.9	0.5	0.9
I_p (ua)				
5	5.5	6.8	2.8	2.0
20	1.9	2.0	1.5	1.6
40	2.0	2.1	—	1.5

a - T.C.'s (Time Constants) in minutes averaged for all runs
b - — indicates no measureable response

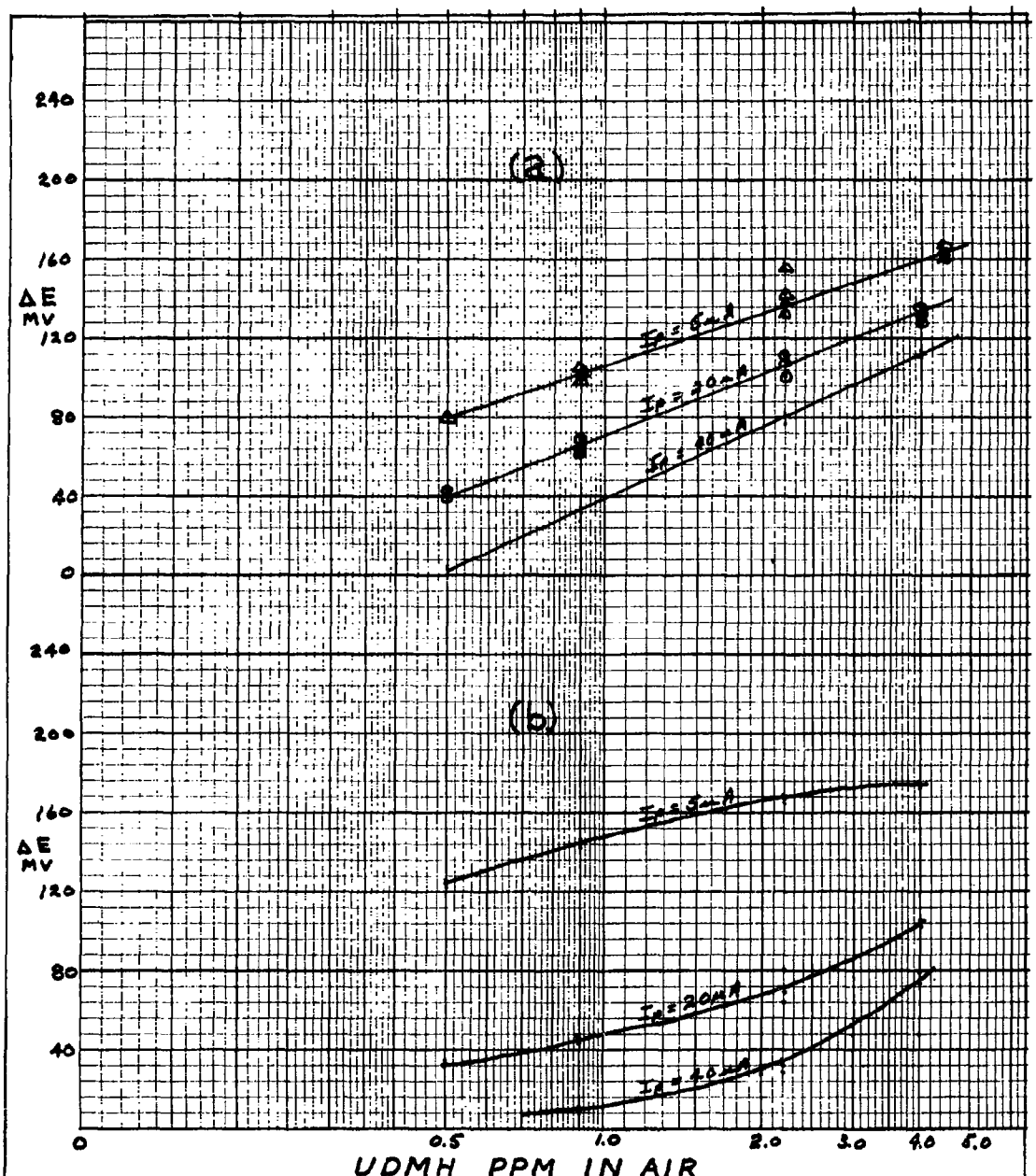

FIG. 10

CHANGE IN CELL VOLTAGE AS A FUNCTION OF UDMH CONCENTRATION FOR I_p's SHOWN IN KI ELECTROLYTE (a) CELL "X" (b) CELL "Y"

TABLE III

Recovery Time Constants for KI Electrolyte

	Cell "X"		Cell "Y"	
	T.C.[a] at UDMH in PPM		T.C. at UDMH in PPM	
	0.5	0.9	0.5	0.9
I_p (ua)				
5	3.4	6.0	4.6	7.1
20	1.5	2.4	2.4	3.6
40	1.3	1.5	—	1.3

a - T.C.'s (Time Constants) in minutes averaged for all runs
b - — indicates no measureable response

The maximum polarization current used in the UDMH tests was 40 microamps to avoid excess depositing of iodine on the outer (+) electrode. Relative values of overvoltage for the deposition of iodine and the other anions is:

I_2/I^-	0.536 volts
Br_2/Br^-	1.065 volts
Cl_2/Cl^-	1.358 volts

These values are based on the hydrogen scale where the potential of hydrogen is considered zero at all temperatures and applied exclusively to solutions at unit activity (Ref 1:413). Even though these values were not observed (as could be expected), they do indicate the order of conversion.

KCl Electrolyte

The characteristic curves for KCl were obtained by the same methods described for KI. However, the voltages recorded varied up to 95 mv for any given value of polarization current under identical test conditions on different days. Table IV shows the deviation encountered at three polarization currents for cell "Y". Since the polarization of the cell was so unpredictable, a complete evaluation of its electrical characteristics was abandoned. However, the response to UDMH was observed and the TLV was detected. Table V shows the response of cell "Y" to UDMH and the blank. Two interesting results can be observed: (1) unlike the other electrolytes, the final response value increased with I_p and (2) the blank was detected about as well as the UDMH. Similar results were obtained with cell "X". Thus, this dip solution is completely unsatisfactory for the requirements of stability and adequate response to the TLV of UDMH.

TABLE IV

Overvoltage deviation with KCl Electrolyte[a]

I_p (ua)	Average E (mv)	Deviation (mv)
5	94	-39 to 56
20	310	-40 to 45
40	469	-17 to 31

a - results of three experimental tests

TABLE V

Response to 0.5 PPM UDMH and Blank in KCl Electrolyte

I_p (ua)	UDMH E (mv)	Blank E (mv)
5	0	5
10	10	13
20	23	15
40	26	25

KBr Electrolyte

The polarization curve for KBr one hour after dipping is illustrated in Fig. 11 - ①. In comparing this curve with that obtained with KI, note that for any given value of I_p, the overvoltage is greater; therefore, the resistance is greater. The effects of time of dip are also shown in Fig. 11 and are quite similar to those obtained with KI. For this reason all test runs were accomplished in the time period between one and four hours after dipping the cell into the electrolyte. The capacitance and AC resistance of the cells were calculated by the same methods used for KI with the results given in Table VI. Note that capacitance is lower with the KBr than KI. However, an additional test was made to see if the cell capacitance would vary with frequency as theory predicted. The results of this experiment (using the circuit shown in Fig. 3-B) are found in Table VII for two frequencies and show a decrease in capacitance with an increase in frequency. The

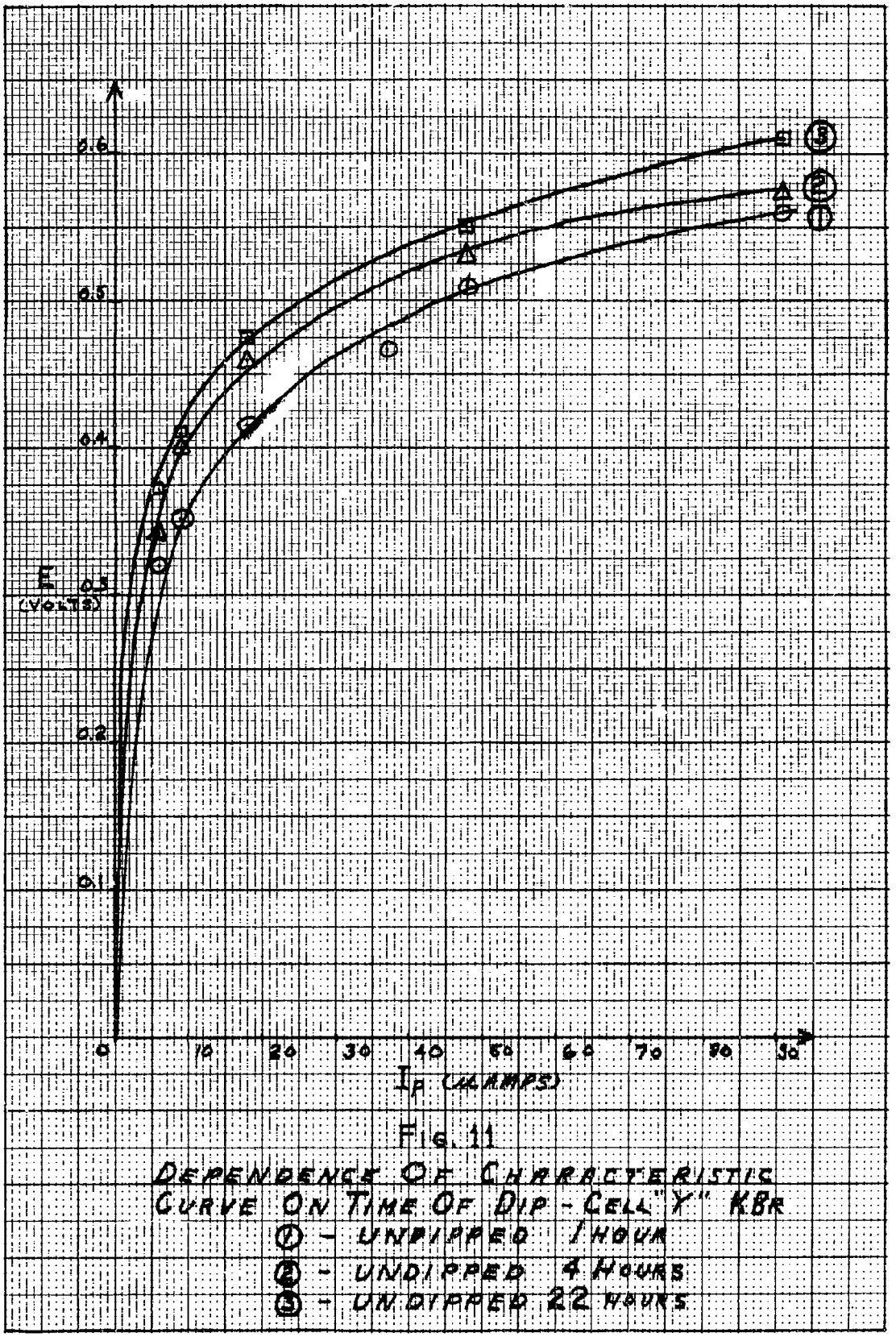

Fig. 11

Dependence Of Characteristic Curve On Time Of Dip - Cell "Y" KBr

① - Unpipped 1 Hour

② - Undipped 4 Hours

③ - Undipped 22 Hours

TABLE VI

AC Resistance and Capacitance of Cells in KBr Electrolyte

T = 22°-25° C. R = 95 ohms Frequency = 60 cycles

	V_{cell} volts	V_R volts	R_{AC} ohms	C microfarads
	0.237	0.975	12.8	139
Cell "X"	0.308	1.23	14.0	137
	0.445	1.84	12.5	138
	0.758	0.417	137	25
Cell "Y"	0.95	0.510	156	32
	1.39	0.810	130	27

TABLE VII

Comparison of Capacitance at Two Frequencies in KBr Electrolyte

Cell "X" T = 22°-25° C. R = 95 ohms

V_{AC} volts	F = 60 cycles C (uF)	F = 80 cycles C (uF)
1.13	139	111
1.414	137	128
2.12	138	123

capacitance of the cell was also determined using an impedance bridge and cell "X". The capacitance decreased to a value of 51 uf at 1,000 cps. An example of the response of the cell to a step current input is given in Appendix B using the cell model. The curve shown in Fig. B-1, Appendix B, compares favorably with the experimental curve obtained from the continuous recorder.

Next, the response to UDMH was evaluated. The experimental results for maximum response can be seen in Fig. 12, for response time constants in Table VIII, and for recovery time constants in Table IX. Response to the blank was negligible. The maximum response was considerably greater and faster for the KBr than the KI. This verifies the theoretical conclusion that a smaller cell capacitance improves response. However, the improvement in response time with the smaller cell (Y) was not as great as for KI. While these analytic determinations were observed, wide variations in the maximum response occurred under similar experimentalconditions. Also, return to a higher reference level occurred. The maximum deviation was +5 mv. This variation was finally attributed to leakage of UDMH through the bleeder valve (Fig. 5) which controlled the rate of flow of the air-UDMH mixture and to loss of the mixture when fresh air entered the system for cell recovery analysis. Rather than design and build a better flow system, it was decided to use the UDMH-NaOH solutions for half the previous runs made at each concentration. Some improvement was realized from this change, but variations were still considerably more than those observed with KI. However, the KI results were

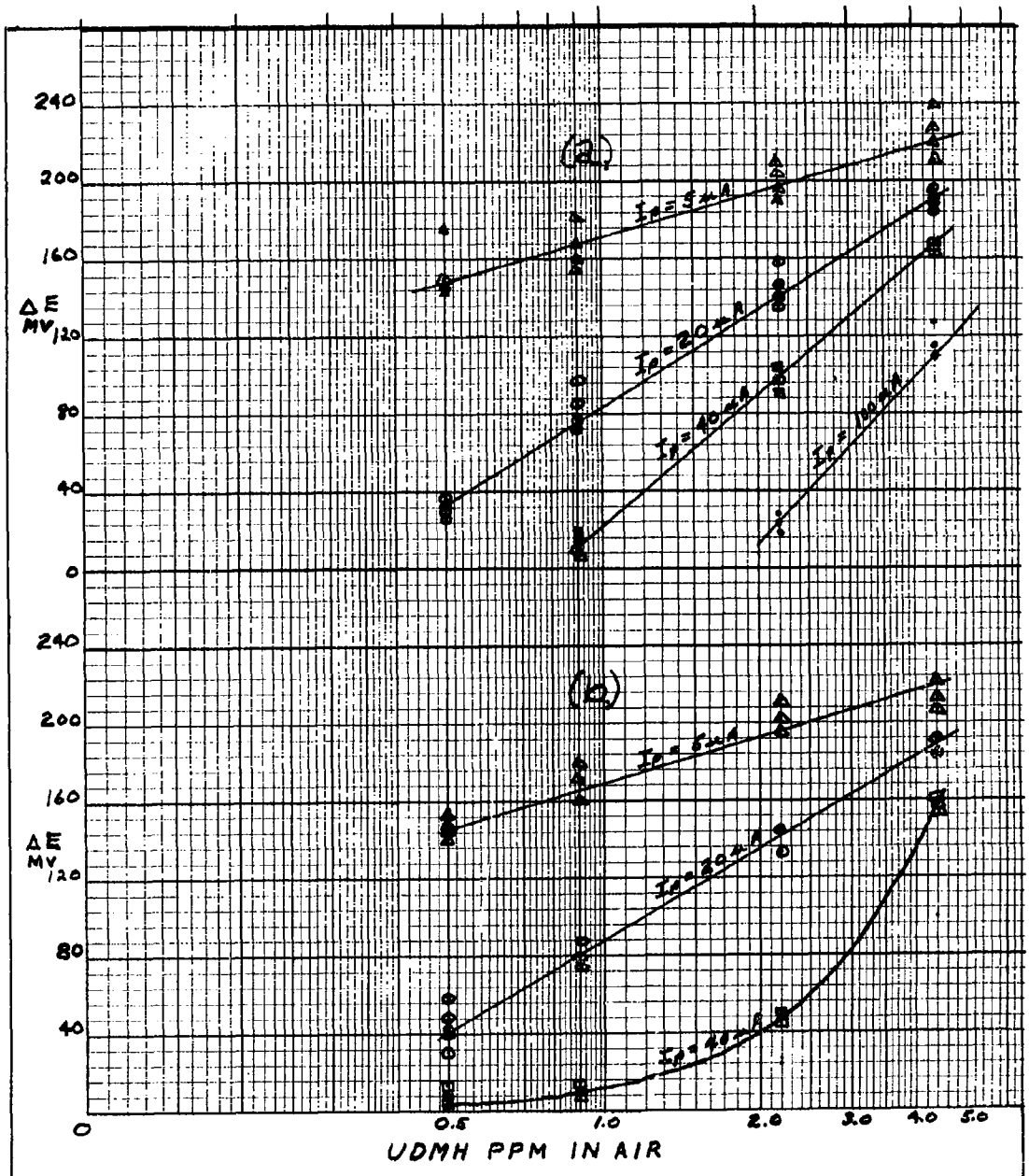

FIG. 12

CHANGE IN CELL VOLTAGE AS A FUNCTION OF UDMH CONCENTRATION

(a) CELL "X" (b) CELL "Y" IN KBR WITH I_p AS INDICATED

TABLE VIII

Response Time Constants for KBr Electrolyte

	Cell "X"		Cell "Y"	
	T.C.[a] At UDMH in PPM		T.C. At UDMH in PPM	
	0.5	0.9	0.5	0.9
I_p (ua)				
5	1.0	1.2	0.9	1.1
20	0.8	1.3	0.7	1.2
40	—	1.6	1.8	1.9

a - T.C.'s (time constants) in minutes averaged for all runs
b - — indicates no measureable response

TABLE IX

Recovery Time Constants for KBr Electrolyte

	Cell "X"		Cell "Y"	
	T.C.[a] At UDMH in PPM		T.C. At UDMH in PPM	
	0.5	0.9	0.5	0.9
I_p (ua)				
5	2.9	4.3	3.5	5.2
20	1.0	0.7	1.1	1.2
40	—	0.4	0.5	0.7

a - T.C.'s (time constants) in minutes averaged for all runs
b - — indicates no measureable response

rechecked at all concentrations previously used. Several minor changes to the previous values obtained were made and are incorporated in the experimental results already discussed for KI.

The fast response and slow recovery with inaccurate return to reference suggested a correction for this problem. An RC differentiator was added to the output of the cell shown in Fig. 3-A. The time constant of the differentiator is designed to be slow with respect to the response but faster than the recovery. Thus, the output is still at an acceptable amplitude for measurement and recovery is rapid. This also results in a zero reference. However, due to time limitations, a complete analysis of this system was not accomplished; but the results indicated that the differentrated pulse was of sufficient time duration to be read on a meter and was rapidly returned to zero (less than one minute at I_p=5ua and 0.5 PPM UDMH).

After the KI electrolyte was rechecked, the response with KBr was investigated again to see what might be causing the rather large variations encountered before. However, the responses measured were considerably higher than the average of those observed previously. The reason for this appeared to be that the cell actually contained a mixture of KBr and KI. At this point, it was decided to conclude the experimental evaluations.

Summary Of Results

The experimental results demonstrated that:

(1) cell capacitance was nearly constant for the different electrolytic systems
(2) cell capacitance decreased with increasing frequency or polarization current

(3) response and recovery improved with a decrease in capacitance
(4) DC resistance decreased with an increase in polarization current
(5) AC resistance is negligible in comparison to the DC resistance
(6) cell "X" had greater capacity and less resistance than cell "Y"
(7) maximum sensitivity to UDMH was obtained with cell "Y"
(8) the KI dip solution was the most accurate of the three electrolytes with respect to response to UDMH and return to reference
(9) adequate baseline stability was obtained for a three hour period with KI.

These results suggested a new model for the cell when exposed to UDMH.

The next chapter discusses this model.

V. UDMH Equivalent Circuit

The negative resistance characteristic with corresponding differences in output voltage for the different cells and electrolytes suggested a piecewise-linear approximation for the cell when exposed to UDMH. A typical voltage response-recovery curve is shown in Fig. 13. The equivalent circuit is shown in Fig. 14. With the exception of the large parallel capacitance and the battery E_A, this circuit is identical to the piecewise-linear model of a triode amplifier. Thus, the cell response to UDMH is analogous to the response of a triode amplifier with a change in input voltage. This model is the same as that given in Chapter II for the electrical equivalent circuit except that the voltage generator, C_U, and the battery, E_A, have been added to account for the cell's electrochemical reaction to UDMH. The primary reason for adding E_A is that it allows use of C_U directly as the PPM concentration of UDMH in air; however, it does have physical meaning since any electrolytic cell exhibits a slight potential difference between electrodes when no external polarization current is applied.

From Fig. 14 we have:

$$E_A + \mu C_U = \left(R_c + \frac{1}{CD}\right) i_1 - \left(\frac{1}{CD}\right) i_2 \qquad (5-1)$$

$$E_s = -\left(\frac{1}{CD}\right) i_1 + \left(R_s + \frac{1}{CD}\right) i_2$$

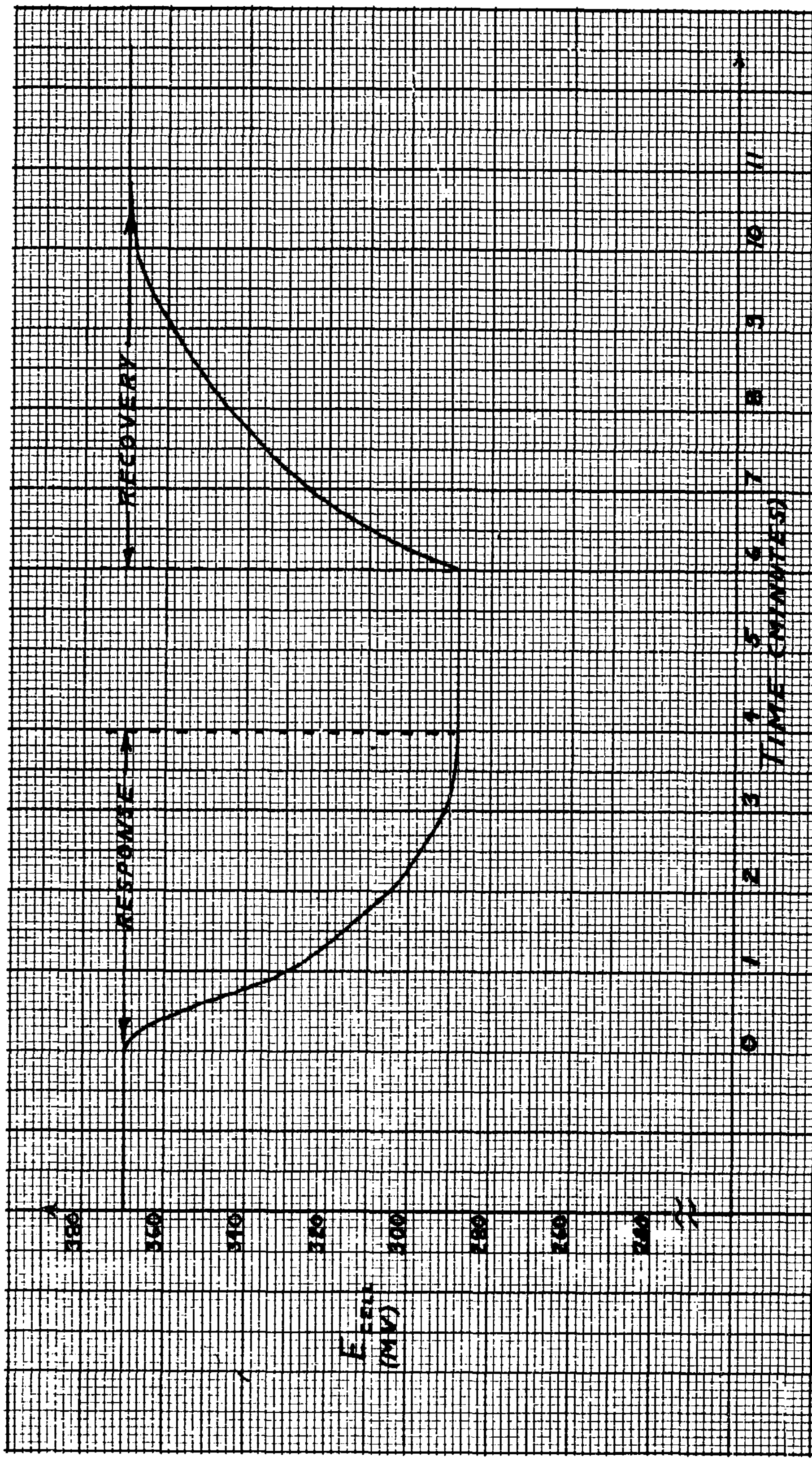

FIG. 13

TYPICAL RESPONSE - RECOVERY CURVE

CELL "Y" KI DIP $I_p = 20\ \mu A$ UDMH 22 PPM

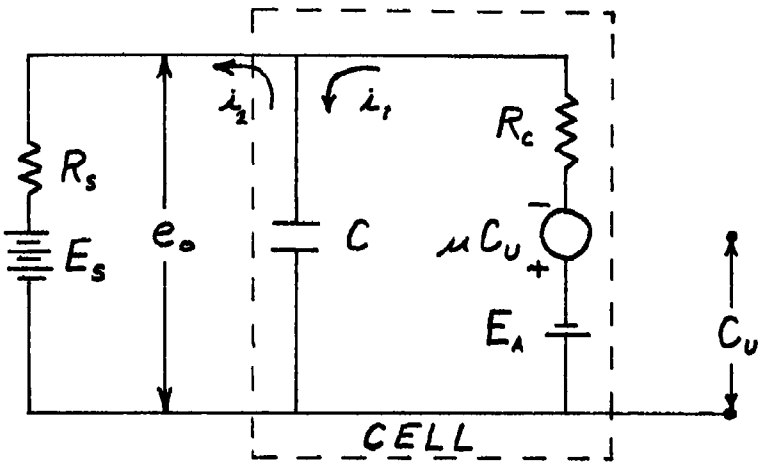

$C_U \equiv$ Concentration of UDMH in PPM
$\mu \equiv$ Amplification Factor
$R_c \equiv$ Cell Resistance
$C \equiv$ Cell Capacitance
$E_s R_s \equiv$ Source Voltage And Resistance Yielding I_p
$E_A \equiv$ Constant for any one I_p

Fig. 14

Cell Equivalent Circuit For UDMH

from which

$$i_1 = \frac{\begin{vmatrix} E_A + \mu C_U & -\frac{1}{CD} \\ E_S & R_S + \frac{1}{CD} \end{vmatrix}}{\begin{vmatrix} R_c + \frac{1}{CD} & -\frac{1}{CD} \\ -\frac{1}{CD} & R_S + \frac{1}{CD} \end{vmatrix}} \qquad (5-2)$$

$$= \frac{E_A R_S + \mu C_U R_S + \frac{E_S + E_A + \mu C_U}{CD}}{R_c R_S + \frac{R_c + R_S}{CD}}$$

$$i_1 = \frac{D\left(\frac{E_A + \mu C_U}{R_c}\right) + \frac{E_S + E_A + \mu C_U}{R_c R_S C}}{D + \frac{R_c + R_S}{R_c R_S C}} \qquad (5-3)$$

The Laplace transform of (5-3) is

$$I_1(s) = \frac{s\left(\frac{E_A(s) + \mu C_U(s)}{R_c}\right) + \frac{E_S(s) + E_A(s) + \mu C_U(s)}{R_c R_S C}}{s + a} \qquad (5-4)$$

where

$$a = \frac{R_c + R_S}{R_c R_S C}$$

hence

$$E_o(s) = I_1(s) R_c - \mu C_U(s) - E_A(s) \qquad (5-5)$$

Substituting (5-4) into (5-5), we have

$$E_o(s) = \frac{s\left(E_A(s) + \mu C_U(s)\right)}{s + a} + \frac{\frac{E_S(s) + E_A(s) + \mu C_U(s)}{R_S C}}{s + a} - \mu C_U(s) - E_A(s) \qquad (5-6)$$

The inverse transform of (5-6) is

$$e_o(t) = -a\left[E_A(t) - \mu C_U(t)\right]e^{-at} + \left[\frac{E_s(t) + E_A(t) + \mu C_U(t)}{R_s C}\right]e^{-at} - \mu C_U(t) - E_A(t) \qquad (5\text{-}7)$$

which is the output voltage as a function of time. The cell reaches a steady state before UDMH (C_U) is applied; therefore, (5-7) can be modified to

$$\begin{aligned} e_o(t) &= E_{ss} - a\left[E_A(t) + \mu C_U(t)\right]e^{-at} \\ &\quad + \left[\frac{E_A(t) + \mu C_U(t)}{R_s C}\right]e^{-at} - \mu C_U(t) - E_A(t) \\ &= E_{ss} - \left[\mu C_U(t) + E_A(t)\right]\left[1 + \left(a - \frac{1}{R_s C}\right)e^{-at}\right] \\ &= E_{ss} - \mu\left[C_U(t) + \frac{E_A(t)}{\mu}\right]\left[1 + \left(a - \frac{1}{R_s C}\right)e^{-at}\right] \qquad (5\text{-}8) \end{aligned}$$

E_{ss} is equal to the final value obtained when $C_U = 0$.

The waveshapes obtained from the experimental data indicate that it takes a finite length of time before the UDMH reaches a steady-state value in the flow system. This length of time is directly proportional to the concentration of UDMH present. This suggests the following type input:

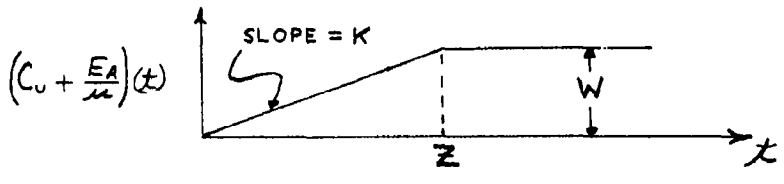

where $\mathcal{Z}$ = time it takes for $(C_U + \frac{E_A}{\mu})(t)$ to reach a steady-state value. This function can be represented by

$$F(t) = K t \left[u(t) - u(t-\mathcal{Z}) \right] + W u(t-\mathcal{Z}) \quad (5-9)$$

WHERE $F = C_U + \frac{E_A}{\mu}$, W = FINAL VALUE OF $F(t)$, $K = \frac{W}{\mathcal{Z}}$

$$u(t) = \begin{cases} 1, & t > 0 \\ 0, & t < 0 \end{cases} \qquad u(t-\mathcal{Z}) = \begin{cases} 1, & t \geq \mathcal{Z} \\ 0, & t < \mathcal{Z} \end{cases}$$

Thus, equation (5-8) becomes

$$e_o(t) = E_{ss} - \mu \left[K t\, u(t) - K t\, u(t-\mathcal{Z}) + W u(t-\mathcal{Z}) \right] \left[1 + \left(a - \frac{1}{R_s C} \right) e^{-at} \right] \quad (5-10)$$

In general, the term $\left(a - \frac{1}{R_s C}\right) e^{-at}$ will be much less than one (even when e^{-at} is maximum) and may be omitted; thus the output is simplified to

$$e_o(t) = E_{ss} - \mu \left[K t\, u(t) - K t\, u(t-\mathcal{Z}) + W u(t-\mathcal{Z}) \right] \quad (5-11)$$

which is a straight line approximation of the output waveshape. Fig. B-2 compares the actual output with that obtained from equation (5-11) for cell "X" in KI electrolyte with a polarization current of five microamps. This linear approximation can also be extended to the cell recovery. However, this will be more accurate with cell "X" than cell "Y" since the recovery of cell "X" is much more linear. The transient recovery of cell "Y" can be observed in Fig. 13. (This is due to a rapid change in R_C at low voltage.)

If only the final value of the cell output voltage is desired, the following equation obtained from the equivalent circuit may be used:

$$e_o = E_s - R_s\left(\frac{E_s + \mu C_U - E_A}{R_s + R_c}\right) \qquad (5-12)$$

This equation was used to obtain the values of ΔE shown in Table X. Also, this table compares the experimental values with the calculated values. The average calculated error is 11.5% or 7 mv of the average experimental value. This is a favorable comparison when the variability in the experimental data is examined. Appendix B (UDMH approximations) contains sample computations using equations (5-11) and (5-12). The next chapter presents conclusions along with recommendations for further study.

TABLE X

Comparison of Calculated ΔE with Experimental ΔE

Cells in KI Electrolyte Exposed to Four Concentrations of UDMH (C_U)

	C_U							
	0.5		0.9		2.2		4.4	
I_p (ua)	C	Ex	C	EX	C	Ex	C	Ex
Cell "X"								
5	80	80	89	97-104	120	130-144	160	160-168
20	45	39-43	54	58-68	82	96-112	130	128-136
40	8	2-5	19	26-33	52	76-83	113	110-114
Cell "Y"								
5	124	122-127	134	142-148	147	166-170	173	171-175
20	32	32-34	39	43-47	60	64-80	94	102-107
40	1	0	10	8-12	33	33-36	73	73-79

- C is computed ΔE in mv
- Ex is experimental ΔE in mv

VI. Conclusions - Recommendations

The basic objective of the problem, i.e. to detect UDMH in the 0.5 to 5.0 PPM range and optimize cell response through analysis of its equivalent electrical parameters, was accomplished. However, accurate repeatability was obtained only with the KI electrolyte. Moreover, this repeatability was achieved only within a time period of from one to four hours after dipping. Although maximum sensitivity was achieved at the low polarization current of five microamps, response and recovery was quite slow. However, a polarization current of twenty microamps with either cell gives adequate sensitivity, in addition to greatly improved response and recovery times. Therefore, continuous, accurate detection of UDMH is possible for a three hour period with either cell using the KI electrolyte at a polarization current of twenty microamps. Also, the output voltage response to UDMH can be predicted by the equations derived from the UDMH equivalent circuit. Finally, this system will give the concentration of less than one PPM of UDMH in air in a matter of minutes as opposed to present laboratory techniques which take approximately eight hours.

The following recommendations for further study are made:

(1) use of the cells with one electrolyte only to eliminate the possibility of a mixture of electrolytes in the cell
(2) further investigation of cell "Y" with the KBr electrolyte and RC differentiator for a small instantaneous detector
(3) investigation of the chemical properties of various KBr electrolytes to eliminate variations in response
(4) investigation of a combination ofKBr and KI as an electrolyte for the possibility of greater, more accurate response for longer continuous detection.

Bibliography

1. Adam, N. K. Physical Chemistry. London: Oxford at the Clarendon Press (1956).

2. Austin, L. G. "Electrode Kinetics and Fuel Cells". Proceedings of the IEEE, 51:820-837 (May 1963).

3. Diamond, L. H. "Unsymmetrical Dimethylhydrazine". Chemical Engineering Progress, 57:87-92 (July 1961).

4. Dole, M. Experimental and Theoretical Electrochemistry. New York: McGraw-Hill Book Co. (1935).

5. Glasstone, S., et al. Theory of Rate Processes. New York: McGraw-Hill Book Co. (1941).

6. Hurd, R. M., et al. Solion Principles of Electrochemistry and Low-Power Electrochemical Devices. Silver Spring, Maryland: Naval Ordnance Laboratory (1957) (AD-143566).

7. Kortum, G. and Bockris, J. O'M. Textbook of Electrochemistry. New York: Elsveier Publishing Co. (1951).

8. Parsons, R. "Equilibrium Properties of Electrified Interfaces". Modern Aspects of Electrochemistry. London: Thomas Butterworth, Ltd (1954).

9. Pinkerton, M. K., et al. A Colorimetric Determination for 1,1 Dimenthylhydrazine in Air, Blood, and Water. ASD Technical Report 61-708 Dayton: Wright-Patterson AFB (December 1961).

10. Potter, E. C. Electrochemistry. New York: MacMillan Co. (1956)

11. Poulos, N. A. Amperometric Propellant-Component Detector. ASD Technical Report 61-154. Dayton: Wright-Patterson AFB (May 1961).

12. Saltzman, B. E. "Preparation and Analysis of Calibrated Low Concentrations of Sixteen Toxic Gases". Analytic Chemistry, 33: 1100-1112 (July 1961).

Appendix A

Determination Of UDMH Concentration In Air

A colorimetric method (Ref 9) is used to determine the concentration of UDMH in PPM in air obtained from bubbling air through a solution of UDMH and NaOH. Referring to Fig. A-1, air flows through the bubbler containing the UDMH solution which in turn flows through the sulfuric acid (H_2SO_4). The flow rate of air through the system is controlled by the calibrated orifice meter, and the total volume of air is indicated on the wet test meter. All of the UDMH in the mixture flowing through the H_2SO_4 is absorbed by it. Trisodium pentacyanoamino ferrate (TPF) is added to the acid coloring it in proportion to the UDMH present. By observing the colored acid with a spectrophotometer, the amount of UDMH absorbed can be calculated. Next, by relating the UDMH absorbed to the volume of air passed through the system (recorded by the wet test meter), the exact concentration of the UDMH in air flowing out of the flask is known. The relationship of the concentration of UDMH in PPM in air versus the concentration of UDMH in 2% NaOH solution on a volume to volume basis is plotted in Fig. A-2. The concentrations used for test purposes lay in a region where the relationship was linear; however, at higher concentrations of UDMH in solution the value in PPM in air is not linear (the slope of the curve decreases). Finally, it is interesting to note that it takes up to eight hours to complete this determination of UDMH at one PPM concentrations or less.

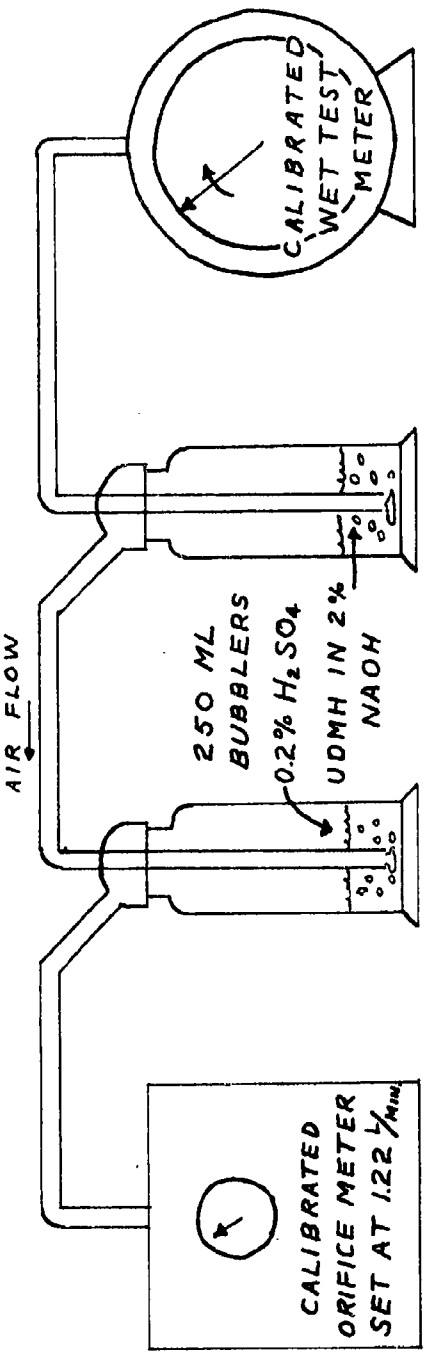

FIG. A 1

APPARATUS FOR THE DETERMINATION OF UDMH IN PPM

FIG A2
CONCENTRATION OF UDMH IN PPM IN AIR VERSUS PER CENT UDMH IN 2% NaOH SOLUTION (Vol/Vol)
PPM UDMH IN AIR
PER CENT UDMH

Appendix B

Sample Calculations

Cell Capacitance

Two methods were selected for experimental determination of cell capacitance. The first method consists of applying an AC sinusoidal voltage across a known resistance and the cell, while the second consists of putting a DC step through the cell, measuring the time constant and from these calculating the capacitance.

AC Method

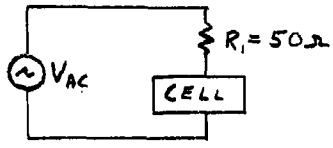

a. Circuit

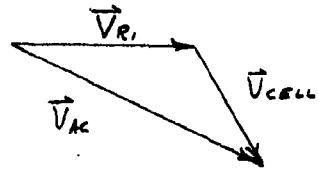

b. Phasor Diagram

From experimental data and phasor diagram (Cell "X"):

$$\vec{V}_{CELL} = 0.325\angle -58^\circ \qquad \vec{V}_{R_1} = 1.2\angle 0^\circ \qquad F = 60 \text{ CYCLES}$$

$$I = \frac{\vec{V}_{R_1}}{R_1} = \frac{1.2}{50} = 24 \times 10^{-3}\,\Omega \qquad (B-1)$$

$$Z_{CELL} = \frac{\vec{V}_{CELL}}{I} = \frac{0.325\angle -58^\circ}{24 \times 10^{-3}} = 13.5\angle -58^\circ\,\Omega \qquad (B-2)$$

Assuming series R and C:

$$Z_{CELL} = R - \frac{j}{\omega C} = 7.15 - j\,11.5 \qquad (B-3)$$

equate real and imaginary terms and solve for C.

$R = 7.15\,\Omega$ $C = 230$ uf If, however, a parallel circuit is assumed, we would have: $Y_{CELL} = G + j\omega C$ (B - 4)

$R = 25\,\Omega$ $C = 165\,\mu F$

DC Method

Using a step I_p (from 40 ua to 50 ua) and either model of Fig. 2 (with R_1 omitted) to find one time constant (TC) we have:

$$TC = \frac{R_s R_2 C}{R_s + R_2} = RC \qquad (B-5)$$

From experimental data:

$$At\ I_p = 40\mu A,\ E_1 = 0.360V;\quad At\ I_p = 50\mu A,\ E_2 = 0.380V$$

$$R_s = 158 \times 10^3 \Omega$$

$$R_2 = 8.75 \times 10^3 \Omega \text{ (averaged over step applied)}$$

$$E_{Tc} = 0.63(E_2 - E_1) \qquad (B-6)$$

$$= 0.63(0.02) = 0.013V$$

$$E_1 + E_{Tc} = 0.373V \quad (At\ T = 1.9^s\ From\ Fig.\ B-1) \qquad (B-7)$$

$$From\ (B-5)\quad R = 0.83 \times 10^4 \quad \therefore TC = 0.83 \times 10^4 C = 1.9$$

$$\therefore C = 229\ \mu F$$

Therefore, the assumption of a series AC equivalent circuit is valid.

From Field Theory

Calculation of capacitance from field theory (Cell "X") is accomplished with the following assumptions:

(1) assume the dielectric constant of the medium between the electrodes is that of the electrolyte
(2) assume the cell is a cylindrical capacitor
(3) assume that the potential of the electrodes are constant over their entire surface.

The capacitance of the cell can be expressed by:

$$C = \frac{2\pi \epsilon L}{\ln b/a} \qquad (B-8)$$

where: $\epsilon_r \approx 70$ for any dip (Ref 7:703)
a = 0.80 cm. (inner radius)
b = 0.96 cm. (outside radius)
L = 0.102 m. (Length)

thus

$$C = \frac{(2\pi)(70)\left(\frac{10^{-9}}{36\pi}\right)(0.102)}{\ln\left(\frac{0.96}{0.80}\right)} \qquad (B-9)$$

$$= 2200\ \mu\mu F$$

This value differs by a factor of approximately 10^5 from the actual values of C determined experimentally.

Characteristic Curve

A curve shwing the comparison between that computed from the cell model and that obtained experimentally is shown in Fig. B-1. From equation (2-8) we have

$$e_o(t) = \frac{E_s R_2}{R_2 + R_s}\left(1 - e^{-\frac{t}{\tau}}\right) \qquad (B-10)$$

Since the experimental data were taken in a region where R is reasonably constant (for more accurate results), equation (B-10) is modified thusly

$$e_o(t) = \left(\frac{E_s R_2}{R_s + R_2} - E_i\right)\left(1 - e^{-\frac{t}{\tau}}\right) \qquad (B-10a)$$

$$\Delta e_o(t) = \Delta E\left(1 - e^{-\frac{t}{\tau}}\right) \qquad (B-11)$$

Since

$$E_1 = 0.360\,V, \quad E_s = 8\,V, \quad R_s = 158\,K\Omega, \quad R_2 = 8.75\,K\Omega$$

$$\Delta E = \frac{(8)(8.75\times10^3)}{166.75\times10^3} - 0.360$$

$$= 0.378 - 0.360$$

$$= 0.018\,V$$

From equation (B-11) the following values were obtained:

at	t (sec)	$\Delta e_o(t)$ (v)	$e_o(t)$ (v)
	0.6	0.0047	0.3647
	1.2	0.0081	0.3681
	2.8	0.0135	0.3735

These values are plotted in Fig. B-1 and compare favorably with the experimental results.

UDMH Approximations

From equation (5-12) we have

$$e_o = E_s - R_s\left(\frac{E_s + \mu C_u + E_A}{R_s + R_c}\right) \qquad (B\text{-}12)$$

From experimentaldata:

$$I_p = 5\,\mu A, \quad R_c = 32\,K\Omega, \quad \mu = 21\ \frac{MV}{PPM}$$
$$E_s = 8\,V, \quad R_s = 1.6\,M\Omega, \quad E_{cell} = 160\,MV$$
$$e_o = 80\,MV \quad FOR\ C_u = 0.5\ PPM$$

Substituting in (B-12) to find E_A we have

$$80 = 8000 - 1.6\times10^6\left(\frac{8000 + (21)(0.5) + E_A}{1.6\times10^6 + 32\times10^3}\right)$$

$$80 = 8000 - 7850 - 0.98\,E_A$$

$$80 = 150 - 0.98\,E_A$$

$$\therefore E_A = \frac{70}{0.98} = 71\,MV$$

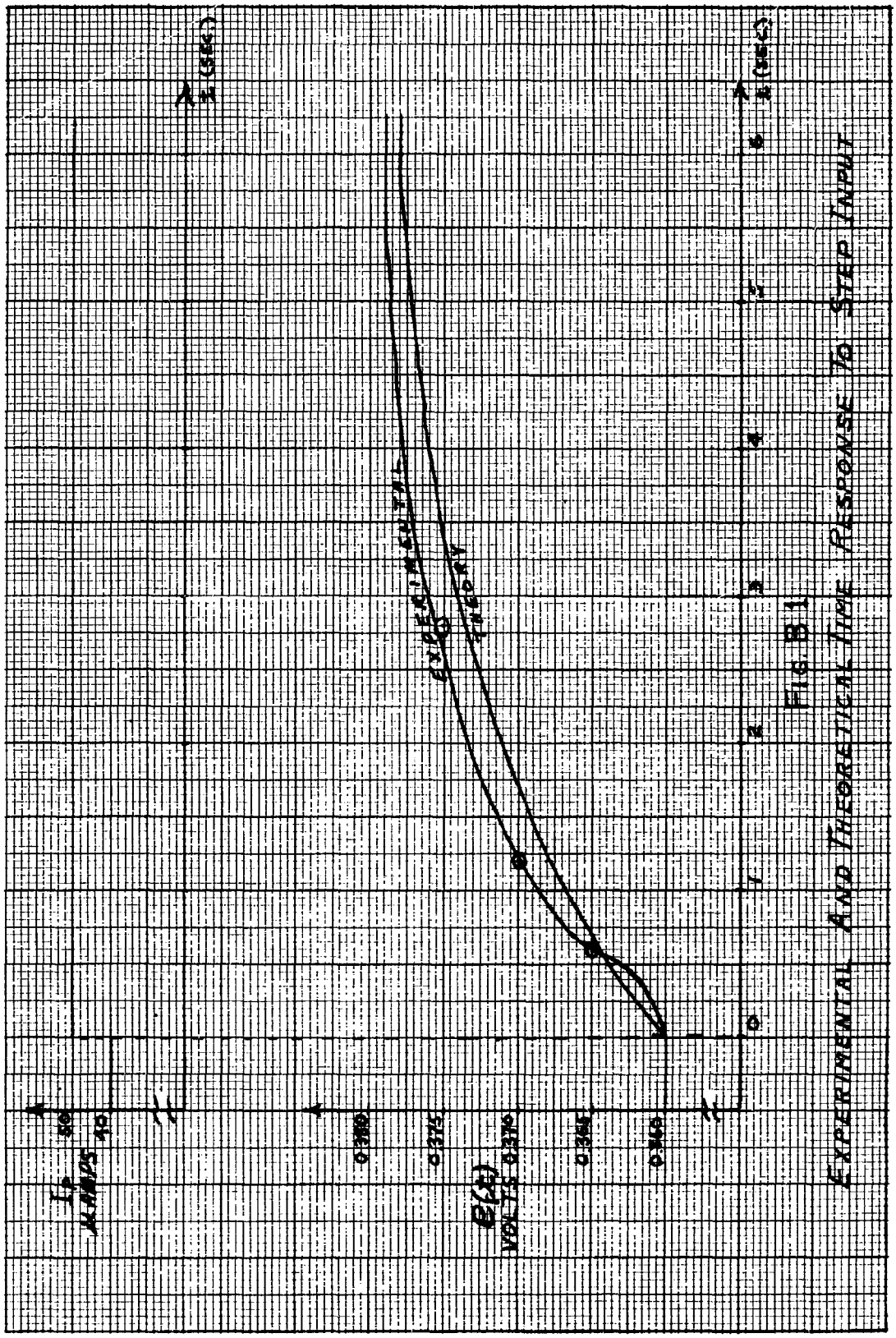

FIG. B.1 EXPERIMENTAL AND THEORETICAL TIME RESPONSE TO STEP INPUT

Now let C_U = 4.4 PPM and substitute in (B-12)

$$e_o = 8000 - 1.6 \times 10^6 \left(\frac{8000 + 21(4.4) + 71}{1.6 \times 10^6 + 32 \times 10^3} \right)$$
$$= 8000 - 8000$$
$$= 0$$
$$\therefore \Delta E = 160 - 0 = 160 \text{ mv}$$

To obtain the time response, equation (5-11) must be used. Therefore,

$$e_o(t) = E_{ss} - \mu \left[K t u(t) - K t u(t-z) + W u(t-z) \right] \quad (B-13)$$

For C_U = 0.5 and the same experimental data as above with z = 600 seconds

$$K = \frac{W}{z} = \frac{C_U + \frac{E_A}{\mu}}{z} = \frac{0.5 + 3.88}{600} \quad (B-14)$$
$$\therefore K = \frac{3.88}{600}$$

Substitute this value in (B-13), to obtain

$$e_o(t) = 160 - 21 \left[\frac{3.88}{600} t u(t) - \frac{3.88}{600} t u(t-600) + 3.88 u(t-600) \right] \quad (B-15)$$

For $t < 600$ sec (B-15) reduces to

$$e_o(t) = 160 - 21 \left(\frac{3.88}{600} \right) t$$

For $t = 0$ $\quad e_o(t) = 160$ mv
$= 60^s$ $\quad = 152$ mv
$= 120^s$ $\quad = 144$ mv

For $t \geq 600$ sec (B-15) reduces to

$$e_o(t) = 160 - 21(3.88)$$
$$= 160 - 81.5$$
$$= 78.5 \text{ mv}$$

which is the final value $e_o(t)$ assumes when exposed to 0.5 PPM UDMH. This value is 1.5 mv less than that obtained experimentally. Fig B-2 shows a comparison between the computed approximation and the experimental curve.

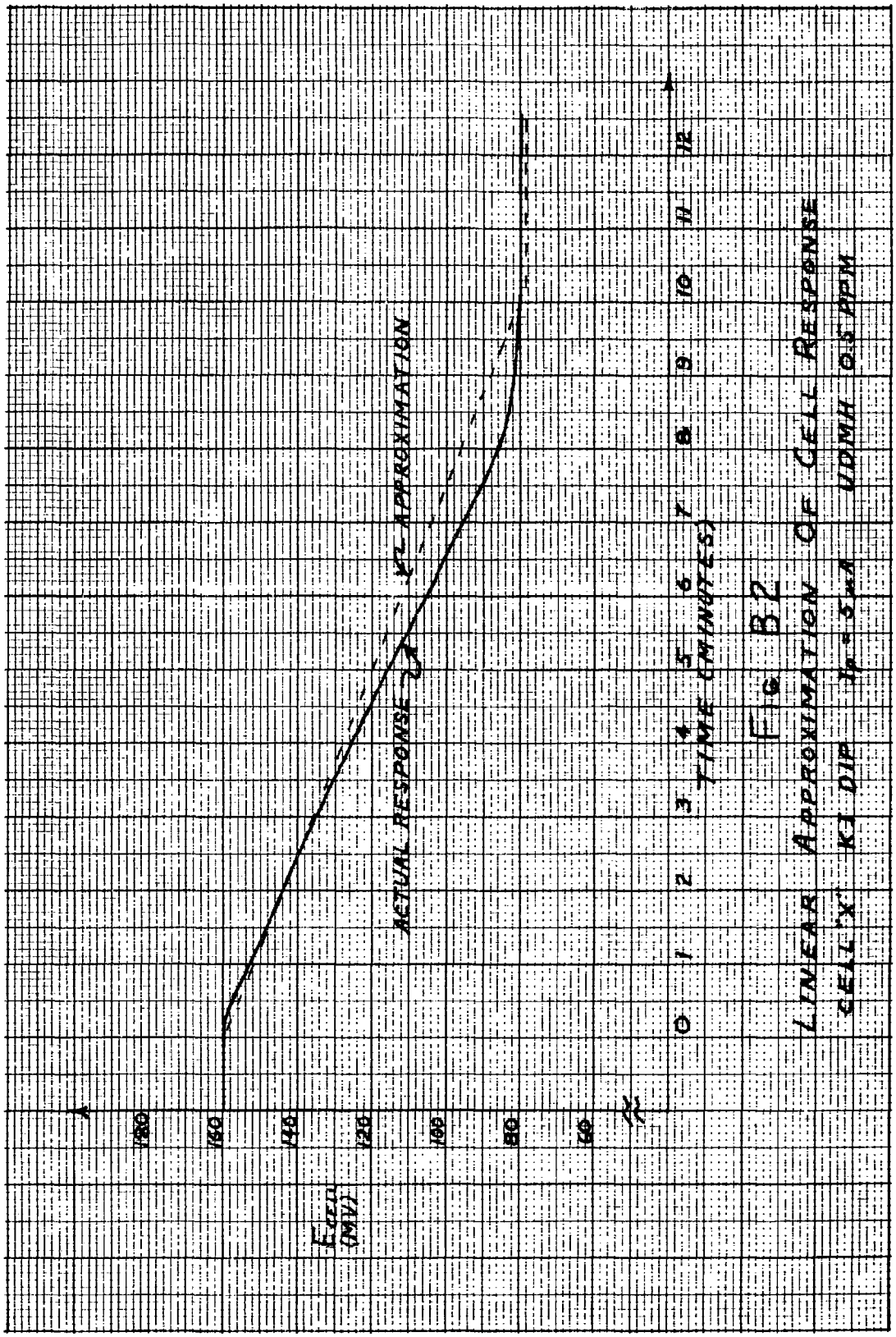

FIG. B2 LINEAR APPROXIMATION OF CELL RESPONSE
CELL 'X' K1 DIP H_p = 3 mA UOMH 0.5 PPM

Appendix C

Construction Of Cells And Composition Of Electrolytic Solutions

Construction of Cell "X"

Cell "X" is constructed in the following manner (Ref 11:3):

(1) Polyethylene tubing of 5/16 inch (in.) diameter is cut to a 13 centimeter (cm) length, and one end is sealed.
(2) Surgical gauze (11 in. by 3 in.) is wrapped around the polyethylene tubing and is secured with thread.
(3) Platinum gauze (3 cm by 4 cm, 99.9% pure) is centered on the surgical gauze and wrapped around it with a 6 in. platinum lead-in wire for electrical connections.
(4) An 8 in. wrapping of 3 in. surgical gauze is wrapped around the inner platinum electrode and fastened with thread.
(5) Another layer of platinum gauze (7 cm by 4 cm) is wrapped around the last layer of surgical gauze and is fastened with platinum wire with a 6 in. lead-in wire attached.

Construction Of Cell "Y"

Cell "Y" is constructed in the same manner as cell "X" except:

(1) The inner electrode (platinum gauze) has dimensions 1.5 cm by 3.5 cm.
(2) The surgical gauze has width 1-1/2 in.
(3) The outer electrode has dimensions 4 cm by 3 cm.

Figure C1 is a picture of the two cells.

Composition Of Electrolytic Solutions

(1) KBr - 100 mL H_2O, 100 mL DEGME (CARBITOL)
16. $NaHCO_3$, 26. KBr

(2) KI - 250 mL H_2O, 250 mL DEGME
6.36. $NaHCO_3$, 156. KI

(3) KCl - 100 mL H_2O, 100 mL DEGME
16. $NaHCO_3$, 1.56 KCl

All three solutions are neutral (ph=7). Carbitol is used to retard drying of the cells while the $NaHCO_3$ is a buffer (it is used to maintain the ph of the solution constant).

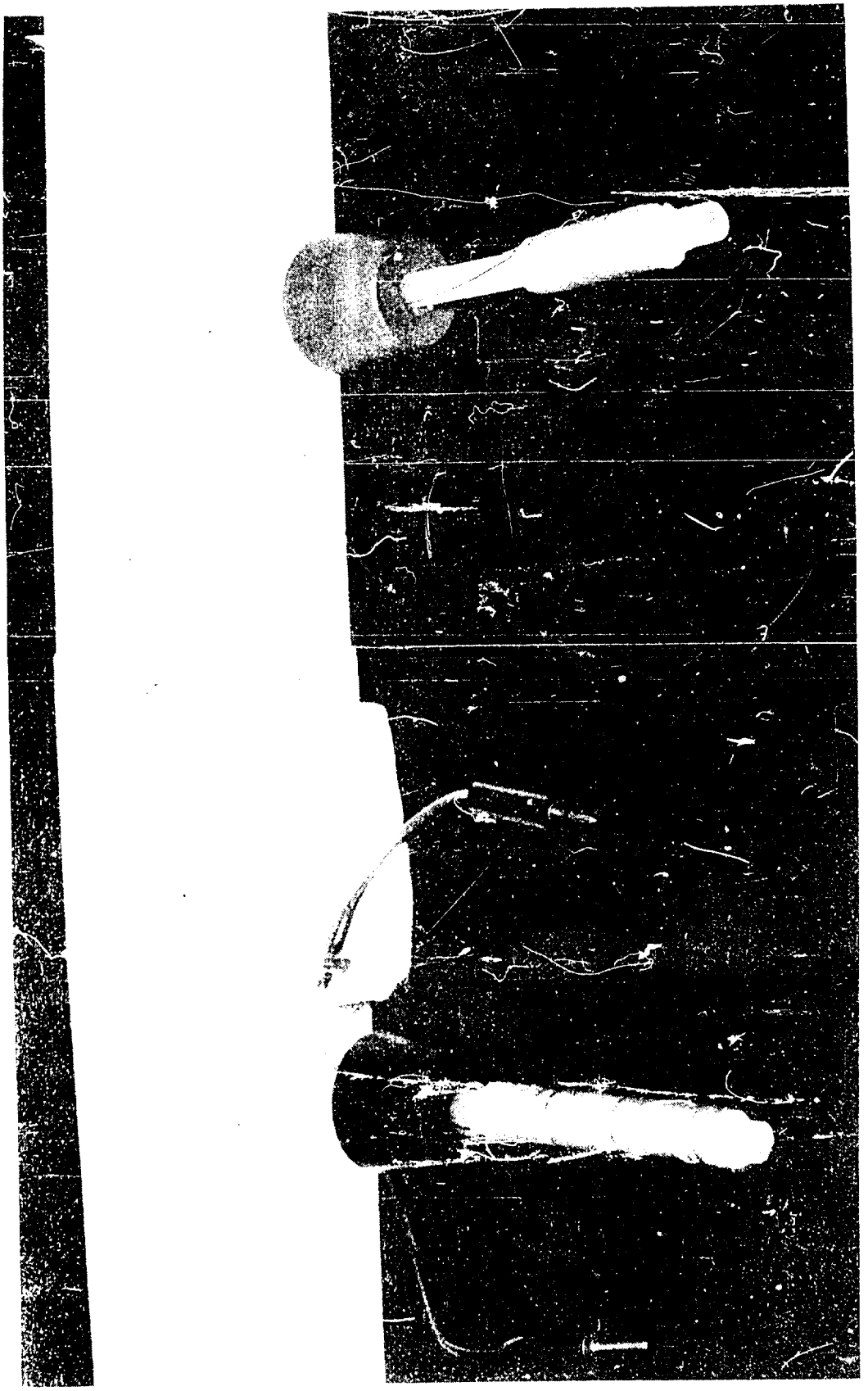

FIG. C1

Appendix D

Optimization Of Cell Parameters

By use of the equivalent model shown in Fig. 2, Chapter II, the cell parameters can be optimized. Assume that the input is a unit step, thus equation (2-8) is modified to be

$$e_o(t) = \frac{R_2}{R_s+R_2}\left(1 - e^{-\frac{t}{\tau}}\right) \qquad (D-1)$$

Now take the derivative of $e_o(t)$ with respect to t

$$\frac{de_o(t)}{dt} = \frac{R_2}{\tau(R_s+R_2)} e^{-\frac{t}{\tau}} \qquad (D-2)$$

Now let $\frac{de_o(t)}{dt} = 0$ thus

$e^{-\frac{t}{\tau}} = 0$ when $e_o(t)$ is a maximum

This will occur when $t = \infty$ or when $\tau = 0$. Since

$$\tau = \frac{R_s R_2 C}{R_s + R_2}$$

cannot be made zero in the physical system, it should be attempted to be made a minimum. This is most easily achieved by making C small since R_s is fixed by the source. Therefore, response time can be improved (decreased) by minimizing C. It is also interesting to note that if R_2 can be made larger ($R_s >> R_2$), the steady-state final voltage will be increased.